Research on Engineering Structures & Materials
www.jresm.org
Research Group

Research Article

Synergistic effect of waste glass powder and exiguobacterium aurantiacum on the mechanical, durability and microstructural performance of bacteria-enhanced geopolymer concrete

Manivannan A [1,a], Kandasamy S [*,1,b], Murugan S [2,c], Vengadesh Marshall Raman J [3,d], Korukonda Jagajjanai Rao [1,e]

[1]*Department of Civil Engineering, Vel Tech Rangarajan Dr. Sagunthala R&D Institute of Science and Technology, Chennai-600062, Tamil Nadu, India*
[2]*Department of Civil Engineering, Government College of Engineering, Dharmapuri, Tamil Nadu, India*
[3]*Department of Civil Engineering, AKT Memorial College of Engineering and Technology, Kallakurichi, Tamil Nadu, India*

Article Info

Article History:

Received 28 Aug 2026

Accepted 19 Oct 2026

Keywords:

Self-healing geopolymer concrete;
Exiguobacterium aurantiacum;
Microbiologically Induced Calcite Precipitation (MICP);
Waste glass powder;
GGBFS;
Fly ash;
SEM;
EDS;
FTIR

Abstract

Waste glass powder (WGP) has emerged as a sustainable geopolymer precursor that reduces industrial waste while enhancing the engineering performance of concrete. In the current study, the effect of WGP on the mechanical and durability properties of bacteria-enhanced geopolymer concrete using Exiguobacterium aurantiacum (MTCC-6414) was investigated. The fresh, mechanical, durability, and microstructural properties were studied for the geopolymer concrete mixtures with different proportions of GGBFS, fly ash, and WGP. Among all mixtures, the geopolymer concrete containing 50% GGBFS and 50% WGP exhibited the best overall performance. The compressive strength of 59.00 MPa and 73.75 MPa was obtained at 28 days and 90 days respectively with an increase of 118.5% and 92.8% over the control mixture. The respective split tensile strengths were 5.06 MPa at 28 days and 5.70 MPa at 90 days, which were increased by 42.5% and 38.7% respectively. The optimum mixture (GBCM7) exhibited a significantly lower rapid chloride permeability value (1493.1 C) compared to the control mixture GBCM0 (2450.5 C), representing a 39.1% reduction in total charge passed, indicating improved resistance to chloride ingress and water penetration. SEM, EDS and FTIR analyses confirmed the formation of a denser geopolymer matrix with improved reaction products attributed to the synergistic effects of reactive silica from WGP and bacterial mineralization.

© 2026 MIM Research Group. All rights reserved.

1. Introduction

The construction industry is one of the largest contributors to global carbon dioxide (CO_2) emissions due to the extensive consumption of ordinary Portland cement (OPC). One ton of cement production releases an amount of CO2 that is equal to one ton, which is a significant contributor to environmental degradation and global warming [1]. Hence, the development of sustainable construction materials with lower carbon footprint is a major research focus. Geopolymer concrete has emerged as an eco-friendly alternative to OPC concrete by utilizing industrial by-products rich in aluminosilicates, such as ground granulated blast furnace slag (GGBFS), fly ash (FA) and

*Corresponding author: drskandasamy@veltech.edu.in
[a]orcid.org/0009-0003-5847-687X; [b]orcid.org/0000-0003-4285-8817; [c]orcid.org/0000-0002=9797-7349; [d]orcid.org/0000-0003-1828-9335; [e]orcid.org/0000-0002-9592-7655
DOI: http://dx.doi.org/10.17515/resm2026-2251ma0828rs

metakaolin, that are activated with alkaline solutions to form a three-dimensional aluminosilicate network [2]. Compared to conventional concrete, the geopolymer concrete has lower greenhouse gas emissions, excellent mechanical strength, superior resistance to chemical attack and better long-term durability. The engineering performance of geopolymer concrete is influenced by the chemical composition and reactivity of the precursor materials. GGBFS provides calcium which promotes the formation of calcium-aluminosilicate-hydrate (C-(A)-S-H) gel, which leads to a rapid strength development under ambient curing conditions. Fly ash contains high silica and alumina which helps in the formation of sodium-aluminosilicate-hydrate (N-A-S-H) gel leading to higher long-term strength and durability. Therefore, the combined use of GGBFS and fly ash has been a common practice in obtaining balanced mechanical properties and durability in geopolymer concrete [3]. Recently, powdered waste glass (WGP) has attracted a lot of attention as a supplementary geopolymer precursor because of its high amorphous silica content and its widespread availability as an industrial waste. WGP addition leads to sustainable waste management and reduces landfill disposal. The waste glass is finely ground and contains reactive silica which actively takes part in the geopolymerization, improves the packing of particles and leads to a denser geopolymer matrix. Previous studies have demonstrated that the incorporation of WGP at suitable substitution levels leads to enhanced compressive strength, reduced chloride penetration and improved water absorption. However, excessive replacement of WGP can reduce the availability of calcium for the formation of the geopolymer gel, thus reducing the mechanical performance [4,5,6]. In addition to optimizing precursor materials, recent research has also focused on the integration of beneficial microorganisms to improve the performance of cementitious materials. Some alkaliphilic bacteria can survive in highly alkaline environment and induce microbial induced calcium carbonate precipitation (MICP).

The precipitated calcium carbonate fills the pores and refines the microstructure, thereby reducing the permeability and improving the mechanical and durability properties of concrete [7]. Among these microorganisms, Exiguobacterium aurantiacum has gained importance due to its ability to tolerate alkaline conditions and to be metabolically active in harsh environmental conditions. These properties render it suitable for geopolymer systems with a strongly alkaline pore solution. Studies on bacteria-enhanced concrete, geopolymer concrete and waste glass powder have been separately investigated. Previous studies have shown that bacterial incorporation improves the matrix densification and durability through biomineralization, while WGP improves sustainability and engineering performance of geopolymer binders [5,8,9,10,11]. However, very little information is available on the use of combined fly ash, GGBFS, powdered waste glass and Exiguobacterium aurantiacum in geopolymer concrete. Moreover, the optimum replacement level of GGBFS with WGP, and the effect of this replacement on fresh, mechanical, durability, and microstructure properties of bacteria enhanced geopolymer concrete have not been investigated thoroughly [12,13]. We hypothesize that a dual-action physicochemical mechanism is in play in this binder: waste glass powder (WGP) has high amounts of amorphous reactive silica (SiO_2 > 70 %), which promotes the geopolymeric dissolution-polycondensation kinetics, yielding higher volumes of sodium/calcium aluminosilicate hydrate (N-A-S-H/C-(A)-S-H) gel matrix, while Exiguobacterium aurantiacum metabolizes organic calcium nutrients via ureolytic hydrolysis to precipitate fine micro-crystalline calcite ($CaCO_3$) directly within residual gel micropores.

This concurrent geopolymer matrix densification and microbial bio-calcification yields a synergistic pore-refinement effect and a significant reduction in ionic diffusivity and improvement in mechanical strength. Hence, the present study aims to investigate the effect of powdered waste glass on mechanical and durability performance of bacteria enhanced geopolymer concrete prepared from GGBFS, fly ash, WGP, and alkaline activators incorporating Exiguobacterium aurantiacum. The systematic assessment of the effect of WGP substitution on consistency, setting time, compressive strength, split tensile strength, flexural strength, rapid chloride permeability, sorptivity and microstructural features using SEM, EDS, FTIR, CFU, and urease activity analyses has been done. The findings of this research add to the knowledge of the responsive effect of bacterial mineralization and waste glass powder on the growth of eco-friendly high performance geopolymer concrete.

2. Experimental Investigation

The current research incorporated GGBFS, waste glass powder, fly ash, Exiguobacterium aurantiacum (MTCC 6414) bacteria & an alkali activator (sodium hydroxide & sodium silicate) mixed along with distilled water to make samples for testing.

Table 1. The physical properties of GGBFS, fly ash, and waste glass powder

Physical Property	GGBFS	Fly Ash	Waste Glass Powder (WGP)
Specific Gravity	2.89	1.97	2.51
Blaine Specific Surface Area (m^2/kg)	335	380	410
Mean Particle Size d_{50} (μm)	12.4	18.6	14.2

2.1 Materials

2.1.1 Ground Granulated Blast Furnace Slag (GGBFS)

Ground Granulated Blast Furnace Slag (GGBFS) is the waste product from the making of iron & steel. It has been made when slag from iron in molten state processed in a blast furnace cools quickly by steaming or through water quenching. A glassy substance was produced by drying and grinding the granular result into a fine powder after quenching. BIS 16714:2018 specification for GGBFS was employed [14]. In this study, it was incorporated at 25%, 50%, 75%, and 100% levels into the total cementitious material. The physical properties and the chemical composition of GGBFS utilized for this study is presented in Table 1 and Table 2 respectively.

2.1.2 Fly Ash

The industrial by-product coming from thermal power plant, fly ash is a fine, grey powder with glassy, spherical particles. Designated as Class F (with a lower CaO percentage) or Class C (with a large CaO percentage). The glass spheres improve the flow and properties of concrete, making it a valuable additive in alkali-activated materials. Indian Standard IS 3812 (Part 1): 2013 for coal fly ash was met by the fly ash that was utilized [15]. This study integrated class C fly ash at amounts of 25%, 50%, 75%, and 100% into the total cementitious material. The research explores the physical properties and the chemical constitution of class C Fly Ash, as detailed in Table 1 and Table 2 respectively.

2.1.3 Waste Glass Powder

Waste glass powder (WGP) is produced by crushing and grinding waste glass into a fine powder. WGP possesses a substantial silica concentration. Finely ground waste glass powder releases reactive amorphous silica, which undergoes pozzolanic and geopolymeric reactions to form supplementary calcium silicate hydrate (C-S-H) and sodium aluminosilicate hydrate (N-A-S-H) gels within the hardened matrix. It can also be utilized to create geopolymer and reduce harmful alkali-silica reactions. In this study, it was incorporated at 25%, 50%, and 75% levels into the total cementitious material. Table 1 and Table 2 illustrates the physical properties and the chemical constitution of Waste Glass Powder (WGP) employed in this investigation respectively.

2.1.4 Fine and Coarse Aggregate

The fine aggregate used for the present work was a manufactured sand (M-Sand) with maximum particle size of 4.75 mm obtained from Uthiramerur, Tamil Nadu, India. It is classified as Zone II as per IS 383:2016 [16] having fineness modulus value of 2.92. The coarse aggregate used was crushed angular stone in two single-sized fractions (12.5 mm and 20 mm) obtained from Uthiramerur, Tamil Nadu, India. The physical and mechanical properties of the concrete are tested according to IS 2386 (Parts 1, 3 and 4). The bulk SSD specific gravity of the fine aggregate was 2.68, the apparent specific gravity was 2.85 and the water absorption was 2.26%. The specific gravities of bulk SSD of 12.5 mm and 20 mm coarse aggregates were 2.76 and 2.79, respectively and the water absorptions were 0.51% and 0.43%, respectively. All aggregates were prepared and batch weighed in the Saturated Surface Dry (SSD) condition and moisture corrections were made during concrete mixing to account for aggregate absorption and free surface moisture.

2.1.5 Alkali-Tolerant Bacteria

Alkali-tolerant bacteria precipitate calcite by raising pH and releasing carbonate ions, which subsequently mix with calcium ions, forming calcium carbonate crystals. The procedure is of immense help for bio-cementation, which enables the bacteria to precipitate calcite into concrete cracks, repairing them. In this present study, Exiguobacterium aurantiacum bacteria were used.

2.1.6 Alkali Activator Solutions

The alkaline liquid to binder ratio was kept constant for all concrete mixtures. The 12M sodium hydroxide (NaOH) solution was prepared by dissolving the commercial grade NaOH pellets (98% purity) [17] in distilled water. The dissolution process is highly exothermic, and therefore the solution was equilibrated to room temperature (25 ±2oC) for 24 hrs. before use. Afterward, the 12 M NaOH solution was well mixed with the commercial liquid sodium silicate (Na2SiO3) contained 29.4% SiO2, 13.7% Na2O, and 56.9% H2O by mass (modulus Ms=SiO2/Na2O=2.15) [18] at a constant mass ratio of 1:3 (Na2SiO3 : NaOH) to prepare the final alkaline activator solution. The combined activator solution was allowed to homogenize to ensure chemical stability prior to being mixed with the precursor materials.

2.1.7 Water

Distilled water was utilized to synthesize the sodium hydroxide (NaOH) solution and dilute the alkaline activator to achieve the targeted 12 M concentration. The prepared NaOH solution was subsequently combined with liquid sodium silicate (Na2SiO3) at a 1:3 mass ratio (SS:SH) to prepare the final alkaline activator solution [19].

Table 2. Percentage chemical composition of Waste Glass Powder, GGBFS and fly ash

Constituents	fly ash	GGBFS	Waste Glass Powder
SiO_2	36.52	32.56	71.10
CaO	28.52	38.91	10.23
Al_2O_3	17.67	16.97	0.94
Fe_2O_3	5.15	1.25	0.16
MgO	4.54	5.13	4.40
Na_2O	0.70	0.20	12.51
K_2O	0.99	0.08	0.31
SO_3	2.37	0.87	0.07
TiO_2	0.58	-	0.07
Cr_2O_3	-	-	0.21
undissolved substance	2.28	4.01	-
combustion loss	0.68	0.02	-

2.2 Bacterial Characterization

Exiguobacterium aurantiacum (MTCC-6414) was procured from Microbial Type Culture Collection (MTCC), CSIR–Institute of Microbial Technology (IMTECH), Chandigarh, India. The strain is a Gram positive, aerobic, rod-shaped bacterium, which can survive under alkaline conditions. The strain was chosen for the current study because of its ability to withstand the alkaline environment of geopolymer concrete and its potential to induce microbiologically induced calcium carbonate precipitation (MICP).

The bacterium produces urease which helps in hydrolysis of urea and promotes calcium carbonate precipitation that is involved in pore refinement and matrix densification. These features make E. aurantiacum a suitable microorganism to improve the mechanical and durability properties of bacteria-enhanced geopolymer concrete. The strain characteristics are taken from the MTCC catalogue. Table 3 presents the morphological and physiological characteristics of Exiguobacterium aurantiacum (MTCC-6414) utilized in the present study.

Table 3. Characterization of Exiguobacterium aurantiacum (MTCC-6414)

Property	Description
Organism	*Exiguobacterium aurantiacum*
MTCC No.	MTCC-6414
Cell morphology	Rod-shaped
Gram reaction	Gram-positive
Oxygen requirements	Aerobic
Habitat	Soil, freshwater, marine sediments
Optimum pH	7.0 to 9.0
Temperature	20 to 30 ^{o}C
Salt tolerance	upto 8%

2.3 Preparation of Bacterial Suspension

The bacterial culture was revived aseptically from the MTCC stock culture in the Biotechnology Laboratory on sterile nutrient broth as the growth medium. Although catalog guidelines recommend a general maintenance temperature of 20–30 °C for Exiguobacterium aurantiacum, an incubation temperature of 37±2oC was deliberately selected to accelerate biomass production kinetics and optimize urease enzymatic expression during the precursor growth phase, consistent with optimal biomineralization protocols reported in literature. After incubation, bacterial cells were collected by centrifugation (5500 rpm) for 15 minutes at 4oC and washed twice with sterile distilled water to remove residual nutrients. The cell pellet obtained was then re-suspended in sterile distilled water to make the bacterial suspension. The preparation procedure of bacterial suspension is shown in Fig. 1. Initially, the bacterial cell concentration was monitored by measuring the optical density (OD) at 600 nm with a UV–visible spectrophotometer, and the viable cell count was then confirmed by the colony-forming unit (CFU) method. A bacterial suspension of 1 × 106 cells/mL was prepared and added in the geopolymer concrete mixes according to the OD and CFU tests. Freshly prepared bacterial suspension was used for each batch to maximize the cell viability during the concrete mixing process.

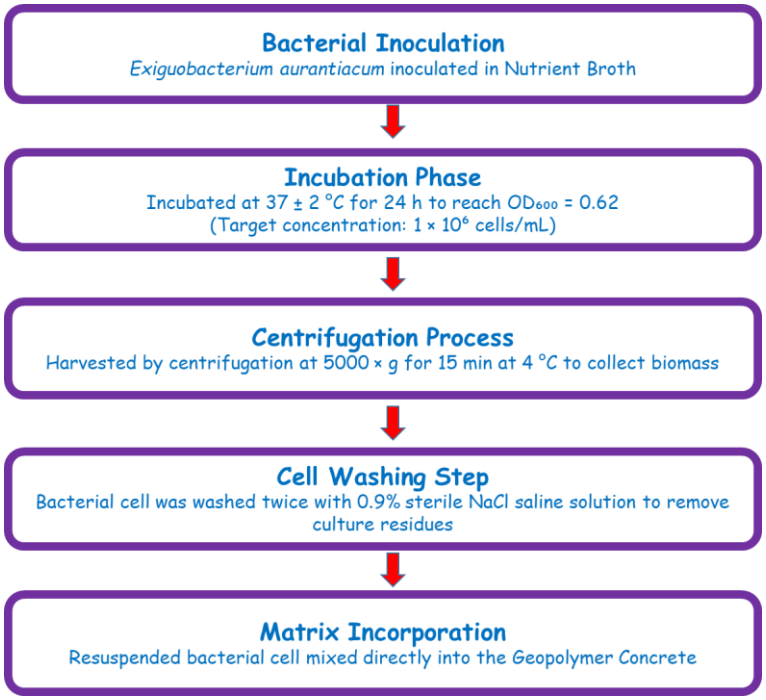


Fig. 1. Schematic flowchart of the bacterial preparation procedure

2.4 Methods

This section analyses various methodologies which were utilized to examine the impact of bacteria, GGBFS, Fly Ash and Waste Glass Powder on bacteria-infused geopolymer concrete.

2.4.1 The Weight Proportion of Bacterial Geopolymer Concrete Mix

The specimens of bacteria-infused geopolymer concrete using an alkali activator solution that had calcium lactate and Exiguobacterium aurantiacum bacteria, coarse aggregate, fine aggregate (M-Sand), waste glass powder, fly ash and Ground Granulated Blast Furnace Slag (GGBFS) with varies weight proportion is shown in Table 4. GBCM0 serves as a conventional Ordinary Portland Cement (OPC Grade 53) control concrete prepared with 460 kg/m^3 cement, a water-to-cement (w/c) ratio of 0.40, and identical aggregate proportions, enabling direct performance benchmarking against standard OPC concrete. To ensure experimental reproducibility, the alkaline activator solution was synthesized using a fixed sodium silicate solution to sodium hydroxide mass ratio (Na_2SiO^3 : NaOH) across all geopolymer mixtures (GBCM1–GBCM8).

Table 4. The composition of bacterial geopolymer concrete

Mix ID	GGBFS (kg/m^3)	Fly Ash (kg/m^3)	Waste Glass Powder (kg/m^3)	Calcium Lactate (kg/m^3)	Alkali-Activator (Molarity)	Bacterial Concentration (cells/mL)
GBCM0	0	0	0	0	0	0
GBCM1	460	0	0	2.3	12	10^6
GBCM2	345	115	0	2.3	12	10^6
GBCM3	230	230	0	2.3	12	10^6
GBCM4	115	345	0	2.3	12	10^6
GBCM5	0	460	0	2.3	12	10^6
GBCM6	230	115	115	2.3	12	10^6
GBCM7	230	0	230	2.3	12	10^6
GBCM8	115	0	345	2.3	12	10^6

Mix ID	Cement (kg/m^3)	F A (kg/m^3)	C A (kg/m^3)	SS (kg/m^3)	SH (kg/m^3)	Extra Water (kg/m^3)
GBCM0	460	621	1041	0	0	184
GBCM1	0	621	1041	52	156	20
GBCM2	0	621	1041	52	156	20
GBCM3	0	621	1041	52	156	20
GBCM4	0	621	1041	52	156	20
GBCM5	0	621	1041	52	156	20
GBCM6	0	621	1041	52	156	20
GBCM7	0	621	1041	52	156	20
GBCM8	0	621	1041	52	156	20

2.4.2 Consistency

To achieve the ideal performance of geopolymer paste, it is essential to determine the optimal alkali activator concentration, for which a consistency test is essential. The test offers the perfect ratio in terms of solution and binder proportion. The mix should not be either too wet or too dry. In order to determine the perfect ratio for geopolymer paste, the apparatus, namely a Vicat with a 10 mm diameter plunger, can be used [20]. It can be taken as a basic procedure to enhance the properties of geopolymer concrete.

2.4.3 Setting Time

The transition of the cementitious material from a plastic state to a solid state can be determined by its setting time and it is assessed using Vicat apparatus. Initial setting shall be checked by inserting needle of 1mm diameter. The final setting time shall be checked by inserting a 5 mm circular cutting-edge needle [21]. For assessing the quality of geopolymer concrete, its setting time is essential.

2.4.4 Compressive Strength

One of the crucial attributes, namely the compressive strength, specifies the effective stress withstanding capacity. For assessing the compressive strength, cubic samples of 100 mm were cast and cured at room temperature. In accordance with IS coding criteria, the specimen was experimented to assess compressive strength after 3, 7, 28, 56 & 90 days curing [22,23].

2.4.5 Flexural Strength

To ascertain the tensile strength of bacterial geopolymer concrete mix, flexural strength analysis is essential. It specifies the ability of a material's binding force. For assessing the flexural strength, the ideal prism specimen with dimensions 150mm x 150mm x 500mm was formulated and subjected to curing at room temperature. In accordance with IS coding criteria, the samples were analysed after a period of 28, 56 & 90 curing days [22].

2.4.6 Split Tensile Strength

Microorganisms enhance the split tensile strength of concrete mix. This parameter is specifically essential for ascertaining a material's capacity to withstand stress. Cylindrical samples with dimensions 100mm in diameter & 200mm height were formulated and allowed to settle down at room temperature to analyze the split tensile strength. The samples were tested after they had been cured under the room temperature for a duration of 3, 7, 28, 56 & 90 days, following IS code criteria [22]. This test evaluates to see if the bacterial geopolymer concrete is strong enough to do the job it was created for.

2.4.7 Rapid Chloride Permeability Test

The rapid chloride permeability testing is developed to determine the resistance of bacterial geopolymer concrete mixes to the movement of chloride ions. This evaluates durability and forecasts corrosion potential of steel reinforcement in chloride conditions. A bacterial geopolymer concrete specimen, moistened with water, is positioned in a test cell and subjected to 60V DC for a duration of six hours. The amount of charge passed (in coulombs) is determined by measuring the current flowing through. Lower charge values indicate better durability and higher resistance to chloride penetration [24]. Test set-up for rapid chloride penetration test as shown in Fig.2.

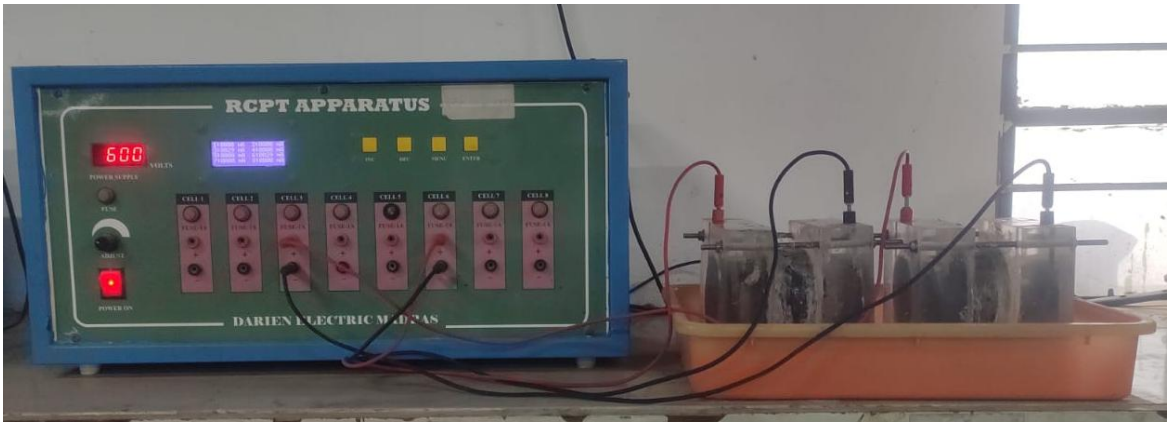


Fig. 2. Test set-up for Rapid Chloride Penetration Test

2.4.8 Sorptivity

In accordance with ASTM C 1585, 100 mm cubes were manufactured and tested [25]. Testing took place over a period of 28 days. Following that, specimens were left to dry for three days at a temperature of 50±2 ◦ C in a thermal oven. These samples were subjected to cooling at ambient temperature before being covered with epoxy, but the suction face remained open. The specimen's initial weight was recorded. Fig. 3 shows the test set-up for sorptivity; the specimens were positioned in a tray on a support so that they were submerged in water 2 to 5 mm deep. Subsequent to absorbing surplus moisture, the specimen was extracted and weighed at predetermined intervals: 1, 5, 10, 20, 30, 60 minutes, then every hour until the sixth hour, then every 24 hours, and

finally every day until the seventh day. The following formula was used to determine the sorptivity (I):

$$(I) = \frac{mt}{a * d} \quad (1)$$

where;

I - represent sorptivity (mm), mt - represent mass of sample (gms) @ time (t), a - represents the sample's exposed area, in mm2, d - represent water density (g/mm3).

Primary and Secondary rates of sorptivity: After line fitting, the slope in the absorption curve, sketched against the square root of time through Least Squares with Linear Regression Analysis, represents an early rate of moisture absorption. From one minute to six hours, the points were plotted. The points are plotted over a period of one to seven days to represent the secondary rate of water absorption consistently.



Fig. 3. Test set-up for sorptivity test

2.4.9 Colony Forming Units (CFU) Assay

The viability of Exiguobacterium aurantiacum (MTCC-6414) in cured geopolymer concrete was assessed by the colony-forming unit (CFU) technique. The concrete specimens were cured for 90 days under ambient conditions and then crushed under sterile conditions. For reducing the external contamination, powder samples were obtained from the inside of each specimen. To 9 mL of sterile physiological saline solution (0.85% NaCl), approximately 1 g of powdered concrete was added and homogenized in a vortex mixer. The suspension was serially diluted to 10-3 and 100 µL of the appropriate dilution was spread on sterile nutrient agar plates. The plates were incubated at 37 ± 2°C for 24–48 h and the colonies were counted. The viable bacterial count was given in colony-forming units per gram (CFU/g) of hardened geopolymer concrete by Eq.

$$CFU/g = \left(\frac{Number\ of\ colonies\ x\ Dilution\ factor}{Volume\ plated(mL) x\ Sample\ weight(g)} \right) \quad (2)$$

2.4.10 Urease Activity Assay

The urease activity of Exiguobacterium aurantiacum (MTCC-6414) was assessed by the colorimetric method to confirm the metabolic activity of the bacterial culture before its incorporation into the geopolymer concrete. Fresh bacterial cultures were grown in a urea-containing medium at alkaline pH. After incubation, the specific urease activity was determined colorimetrically by measuring the concentration of released ammonium ions at 420 nm (OD420) using Nessler's reagent as the colorimetric indicator. The absorbance values obtained were used as indicators of urease activity, where a higher absorbance indicated a higher urease activity and improved bacterial metabolic performance. The experimental setup for the urease activity analysis is shown in Fig. 4.



Fig. 4. Test setup for urease activity analysis of bacterial geopolymer concrete

3. Results and Discussion

3.1 Consistency

The consistency test was conducted to study the influence of powdered waste glass (WGP) on the water demand of the bacteria-enhanced geopolymer binder. Fig. 5 shows the consistency values of all mixtures. The control mixture (GBCM0) had a consistency of 34% but the values of consistency ranged from 30% to 35% in the presence of WGP. The consistency of GBCM2 was the lowest (30%) and the consistency of GBCM6 was the highest (35%) among all mixtures. The best combination, 50% GGBFS and 50% WGP (GBCM7), achieved a consistency of 33%, which was very close to the control blend. The minor difference in consistency indicates that the replacement of GGBFS with WGP had a marginal effect on the fresh properties of the geopolymer binder. This behavior is attributed to the smooth and non-porous surface texture of the finely ground waste glass particles, which alters the particle packing and rheological behavior of the geopolymer paste. In addition, the high amorphous silica content of WGP is beneficial for geopolymerization without significant increment in water demand [26,27,28]. The effect of WGP on workability and setting characteristics of geopolymer binders due to the change of Si/Al ratio and particle packing have been reported in previous studies. Satisfactory fresh properties are obtained at suitable replacement levels.



Fig. 5. Comparison of consistency of geopolymer paste mix

The consistency value obtained for the optimum mixture was 33% which shows the addition of 50% WGP had no adverse effect on the fresh properties of the geopolymer binder. In the binary GGBFS–Fly Ash mixtures (GBCM1–GBCM5), increasing Fly Ash content systematically improved mixture workability and reduced liquid demand. GBCM2 (75% GGBFS + 25% Fly Ash) displayed a

consistency increase compared to GBCM1 (100% GGBFS) due to the spherical morphology of Fly Ash particles, which induce a ball-bearing effect, lowering inter-particle friction. In contrast, substituting GGBFS with Waste Glass Powder (WGP) in GBCM6–GBCM8 altered consistency based on angular particle geometry and surface area. While moderate WGP replacement (GBCM7: 50% GGBFS + 50% WGP) maintained favorable flow properties, higher replacement levels increased liquid demand due to angular fragment friction. This suggests that the combined use of GGBFS, fly ash and WGP resulted in a binder system with sufficient water requirement for concrete production. In addition, no visible adverse effect on the consistency of the geopolymer paste was caused by the bacterial suspension of Exiguobacterium aurantiacum, indicating compatibility of bacterial inclusion with the fresh-state behavior of the binder. The similar consistency, along with the significant improvements in mechanical strength and durability, confirm the optimized binder composition provides a balanced geopolymer matrix for sustainable construction applications.

3.2 Setting Time

The initial and final setting times of the bacteria-enhanced geopolymer binder mixtures are presented in Fig. 6. The initial setting time of the control mixture (GBCM0) was 35 min, and the final setting time was 365 min. Across all evaluated geopolymer mixtures, the initial setting time varied from 27 to 377 min, and the final setting time ranged between 298 and 530 min. Among the GGBFS–Fly Ash binary systems (GBCM1–GBCM5), GBCM1 (100% GGBFS) exhibited the shortest initial and final setting times (27 min and 298 min, respectively), whereas increasing the Fly Ash replacement level (up to GBCM5) systematically extended the setting times up to 377 min (initial) and 530 min (final). The optimum blend, GBCM7 (50% GGBFS and 50% WGP) showed initial and final setting times of 48 min and 328 min, respectively, indicating a balanced setting behaviour suitable for practical concrete applications. The change in setting time is mainly related to the chemical composition and reactivity of the geopolymer precursor materials. GGBFS has relatively high calcium content, this makes dissolution process fast, so calcium-aluminosilicate-hydrate (C-(A)-S-H) gel is formed rapidly and setting time is reduced. On the other hand, WGP is mainly amorphous silica with relatively less calcium, so the geopolymerization reaction is slower at higher replacement levels. Therefore, the increase of the WGP content beyond the optimum ratio delays the formation of the products of the reaction and increases the initial and final setting times. Similar findings have been reported that ground WGP affects the dissolution kinetics and setting properties of alkali-activated binders [29,30]. Likewise, other researcher observed that the setting time is extended with increased content of silica-rich precursor in the alkali-activated slag systems due to slower reaction kinetics [31].

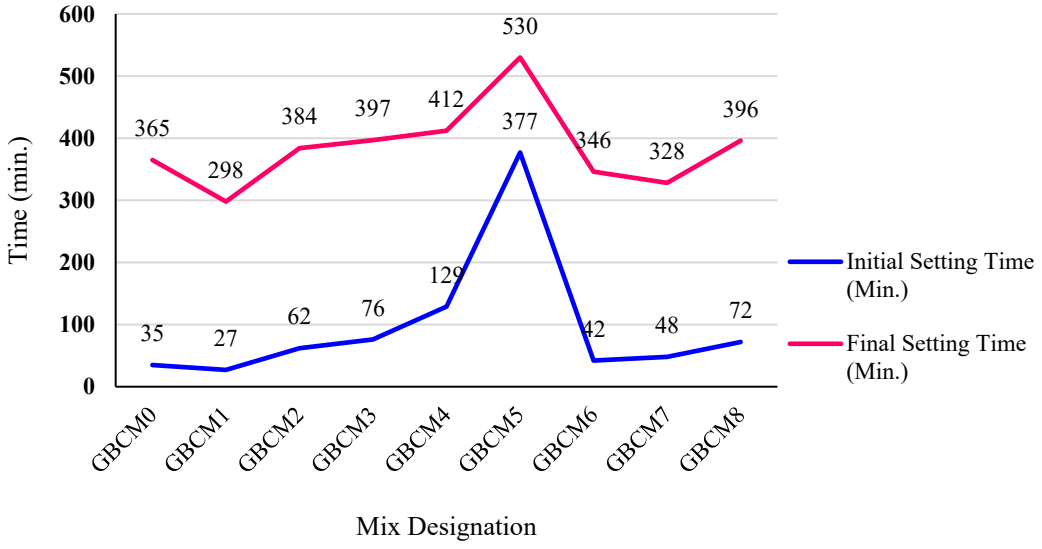


Fig. 6. Comparison of initial & final setting time of geopolymer paste mix

The setting behavior of GBCM7 shows that substituting 50% of GGBFS by WGP provides a good compromise between workability and hardening characteristics. The initial setting time was slightly higher than the control mixture but the final setting time was still lower than the mixtures

with higher setting times. This allows enough time for mixing, transportation and placement without adversely affecting the early strength development. This balanced behavior is due to the combined effects of calcium supplied by GGBFS and reactive silica contributed by WGP, which promote the simultaneous formation of C-(A)-S-H and sodium-aluminosilicate-hydrate (N-A-S-H) gels. Furthermore, the existence of Exiguobacterium aurantiacum did not lead to excessive retardation of the setting process, suggesting that the bacterial suspension was compatible with the alkaline geopolymer system. Similar findings reported, concluding that the interaction between calcium-rich and silica-rich precursors governs the setting behavior and microstructural development of geopolymer binders [27]. Overall, the results of the setting time show that the incorporation of WGP affects the kinetics of geopolymerization and the optimum 50% GGBFS–50% WGP binder composition provides appropriate fresh state characteristics together with the superior mechanical strength and durability reported in this study.

3.3 Compressive Strength

The compressive strength of bacteria enhanced geopolymer concrete (BGPC) mixtures at different curing ages are shown in Fig. 7. All mechanical property tests, including compressive strength evaluations across 3, 7, 28, 56, and 90 days of ambient curing, were conducted in triplicate (n=3) to ensure statistical reliability. The control concrete (GBCM0) showed a compressive strength of 38.25 MPa at 90 days of age. All the GGBFS-based geopolymers exhibited higher strength. For the studied mixtures, the highest compressive strength was obtained for GBCM7 (50% GGBFS + 50% WGP) with 23.60, 42.35, 59.00, 64.85, and 73.75 MPa at 3, 7, 28, 56, and 90 days, respectively, which is about 93% higher than the control at 90 days [23]. Whereas, 100% fly ash mix (GBCM5) showed the lowest strength (8.25 MPa at 90 days) which indicated the low reactivity of fly ash under ambient curing conditions. When partially replaced by fly ash, a progressive reduction in compressive strength was observed. The addition of waste glass powder (WGP) led to a significant enhancement in the mechanical performance especially in GBCM6 and GBCM7. The synergistic effect of GGBFS and WGP results in better performance of GBCM7. The high Ca content of GGBFS promoted the formation of C-(A)-S-H gel, while the amorphous silica released from WGP induced further geopolymerization, leading to a denser binder matrix. The balanced Ca/Si ratio of GBCM7 led to the development of interconnected C-(A)-S-H and N-A-S-H gels, improving load transfer and reducing internal porosity [27,32]. On the other hand, the increased fly ash content led to a decreased calcium availability and retarded the geopolymerization reaction leading to lower compressive strengths. Similarly, the strength was also decreased when WGP was used to replace excessive GGBFS (GBCM8) due to lack of calcium to form calcium rich reaction products.

The presence of bacteria further improved the compressive strength by microbial induced calcium carbonate precipitation (MICP). The CFU analysis indicated that Exiguobacterium aurantiacum was viable before incorporation, thereby confirming its active role in biomineralization. The precipitated $CaCO_3$ in pores and microcracks could help to obtain a refined pore structure and a stronger interfacial transition zone. The improved strength of the optimized mixture could be due to the synergistic effects of geopolymer gel formation and bacterial mineralization [27,33,34]. The results obtained demonstrated that the substitution of fly ash with waste glass powder leads to a significant improvement in the mechanical performance of bacteria-enhanced geopolymer concrete at room temperature. The optimal binder composition was 50% GGBFS and 50% WGP (GBCM7), confirming the importance of an adequate balance between calcium and silica rich precursors combined with bacterial biomineralization to produce a dense geopolymer matrix with improved compressive strength. Because bacterial concentration was kept constant (1x106 cells/mL) across all geopolymer mixtures (GBCM1–GBCM8), strength gains reflect combined matrix densification (geopolymerization) and MICP biomineralization. The absence of a corresponding bacteria-free control series is acknowledged as an experimental limitation; hence, individual performance gains cannot be exclusively isolated to bacterial activity. These results are in agreement with previous studies showing that the combination of GGBFS with reactive silica sources promotes the formation of geopolymer gel and improves the long-term mechanical performance of alkali-activated materials [35].

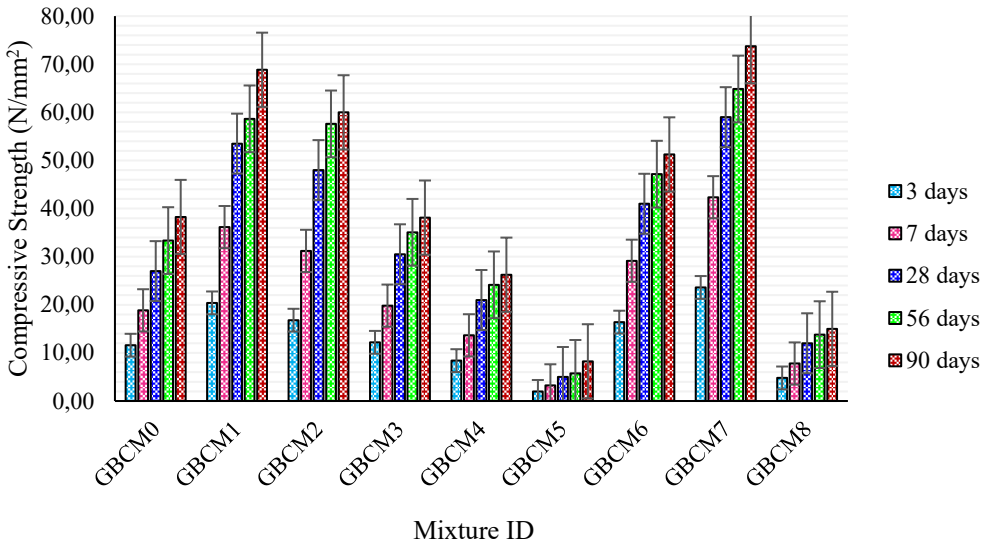


Fig. 7. Comparison of compressive strength of bacterial geopolymer concrete

3.4 Flexural Strength

The flexural strength of the bacteria-enhanced geopolymer concrete (BGPC) mixtures at 28, 56, and 90 days is presented in Fig. 8. The flexural strength evaluations across 28, 56, and 90 days of ambient curing, were conducted in triplicate (n=3) to ensure statistical reliability. The ratios of GGBFS, fly ash (FA) and waste glass powder (WGP) have a significant influence on the flexural behavior. Among the mixtures studied, GBCM7 with 50% GGBFS and 50% WGP exhibited the highest flexural strength of about 5.30, 5.80, and 6.00 MPa at 28, 56, and 90 days, respectively. GBCM7 exhibited an improvement of about 43% compared to the control concrete (GBCM0) which reached 4.20 MPa at 90 days. The 100% fly ash mixture (GBCM5) on the other hand showed the lowest flexural strength (2.00 MPa at 90 days) indicating the limited effectiveness of fly ash as the sole geopolymer precursor at ambient curing. The enhanced flexural performance of GBCM7 is due to the synergistic interaction of GGBFS and WGP. The calcium from GGBFS promoted the rapid formation of C-(A)-S-H gel, while the reactive amorphous silica from WGP helped the formation of more N-A-S-H gel. These reaction products co-existed to develop a dense and homogeneous geopolymer matrix with better bond between aggregate and paste. Moreover, the CFU analysis confirmed the viability of Exiguobacterium aurantiacum, providing active microbial-induced calcium carbonate precipitation (MICP). The precipitated CaCO3 filled the pores and microcracks, contributed to strengthening of the interfacial transition zone and retarded the crack propagation under flexural loading thus improving the overall flexural resistance of the composite [32]. The binary GGBFS mixture (GBCM1) also showed a relatively high flexural strength of about 5.80 MPa at 90 days, indicating the beneficial effect of the calcium-rich precursor on geopolymerization. However, the flexural strength was gradually decreased with the increase of fly ash content. GBCM2, GBCM3 and GBCM4 showed flexural strengths of 5.50, 4.40 and 3.60 MPa respectively at 90 days. The decrease was attributed to the lower availability of calcium and the slower kinetics of fly ash reaction, which hindered the formation of calcium-rich binding phases during ambient curing. The ternary mixture GBCM6 achieved 5.10 MPa after 90 days, which indicated the positive effect of partial replacement of fly ash with WGP on the development of geopolymer gel and flexural behavior. On the other hand, flexural strength reduced to about 2.80 MPa for the 75% WGP content (GBCM8) which indicated that large replacement of GGBFS caused lack of calcium for optimum binder development. In general, the flexural strength results followed a similar trend as those observed for compressive and split tensile strengths, confirming that the mechanical performance of bacteria-enhanced geopolymer concrete is governed by the balance between calcium-rich and silica-rich precursors. The best 50% GGBFS-50% WGP binder system (GBCM7) showed the highest flexural strength owing to the synergistic effects of increased geopolymer gel formation and bacterial biomineralization. The enhanced crack resistance and the increased interfacial bonding result in a more compact and durable geopolymer matrix. The results are in line with the previous

studies which have shown that the incorporation of GGBFS and waste glass powder enhances the flexural behavior through the refinement of the microstructure and strengthening of the geopolymer network, while bacterial MICP helps in crack bridging and pore refinement.

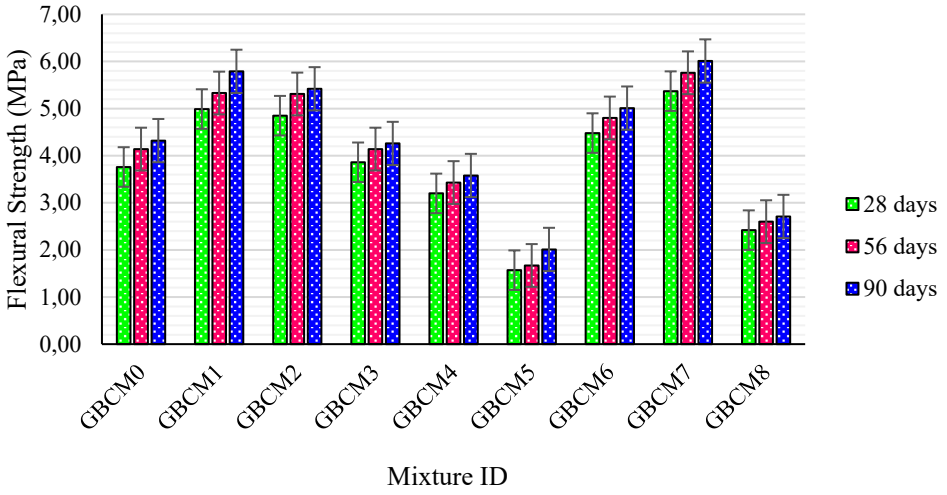


Fig. 8. Comparison of flexural strength of bacterial geopolymer concrete

3.5 Split Tensile Strength

The split tensile strength of bacteria-enhanced geopolymer concrete (BGPC) mixtures at different curing ages is shown in Fig. 9. The flexural strength evaluations across 3, 7, 28, 56, and 90 days of ambient curing, were conducted in triplicate (n=3) to ensure statistical reliability. The GGBFS, fly ash (FA) and waste glass powder (WGP) contents had a significant effect on the tensile performance. The optimized geopolymer mixture (GBCM7) attained a 90-day split tensile strength of 5.70 MPa, representing a 39.0% improvement over the control OPC concrete GBCM0 (4.10 MPa). On the other hand, the mixture with 100% fly ash (GBCM5) showed the lowest tensile strength (1.95 MPa at 90 days), which indicates its limited reactivity under ambient curing conditions. The higher tensile performance of GBCM7 is attributed to the synergism of GGBFS and WGP. The high calcium content of GGBFS contributed to the formation of C-(A)-S-H gel and the reactive amorphous silica from WGP contributed to the formation of N-A-S-H gel, which resulted in a compact and well-connected geopolymer matrix. The balanced precursor composition enhanced the interfacial bond between paste and aggregates which led to higher resistance to crack initiation and propagation under indirect tensile load. Moreover, the confirmed viability of Exiguobacterium aurantiacum by the CFU analysis indicates the active role of the bacterial cells in Microbial Induced Calcium Carbonate Precipitation (MICP). The CaCO3 precipitate occupied the microvoids and microcracks, refined the pore structure and strengthened the interfacial transition zone, leading to enhanced tensile behavior [33,34]. The binary mixture of GGBFS (GBCM1) also showed high tensile strength, about 5.50 MPa at 90 days, due to the rapid formation of calcium-rich reaction products. However, the tensile strength was gradually decreased with the replacement of GGBFS with increasing amount of fly ash. The split tensile strength of GBCM2, GBCM3 and GBCM4 at 90 days was 5.10, 4.05 and 3.40 MPa respectively. The reduction is attributed to the lower calcium availability of fly ash which hinders the geopolymerization as well as the development of calcium-rich binding phases under ambient curing. The ternary mixture GBCM6 showed higher tensile strength of 4.70 MPa than the fly ash-rich mixtures, which suggests that the partial substitution of fly ash by WGP can effectively promote the formation of geopolymer gel. However, the tensile strength decreased to 2.50 MPa when the WGP content increased to 75% (GBCM8), which indicates that excessive substitution of GGBFS leads to insufficient calcium for optimum binder development. The split tensile strength results generally followed the same trend as compressive strength, which confirmed that the mechanical performance of bacteria-enhanced geopolymer concrete depends on an optimum balance of calcium-rich and silica-rich precursors. The 50% GGBFS–50% WGP binder system (GBCM7) showed the highest tensile strength due to the synergistic effects of the enhanced geopolymerization and bacterial biomineralization resulting in improved crack

resistance and a more compact microstructure. The results are in agreement with previous studies, which reported that GGBFS and waste glass powder improved the tensile performance by enhanced gel formation and pore refinement and bacterial MICP further improved the geopolymer matrix by reducing internal defects.

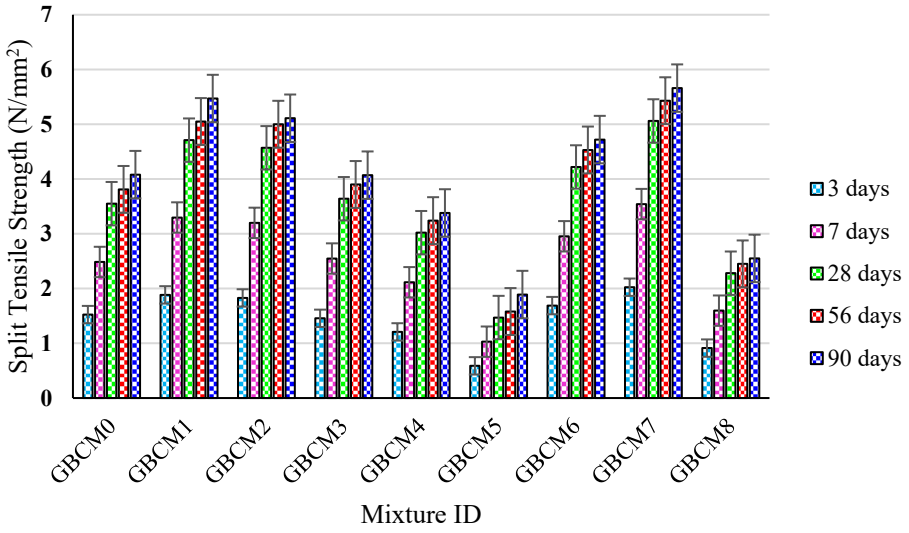


Fig. 9. Comparison of split tensile strength of bacterial geopolymer concrete

3.6 Rapid Chloride Permeability Test

The results of the rapid chloride penetration test (RCPT) for bacteria enhanced geopolymer concrete (BGPC) mixes are presented in Fig. 10. The resistance to chloride ion penetration was determined on the basis of the total charge passed through the concrete specimens in coulombs as per ASTM C1202. Results show that the binder composition has a strong effect on the chloride permeability of geopolymer concrete. RCPT charge passed and ASTM C1202 chloride permeability classification as shown in Table 5.

Table 5. RCPT charge passed and ASTM C1202 chloride permeability classification

Mix ID	Total Passed Charge (C)	ASTM C1202 Permeability Class	Percentage Change relative to GBCM0 (%)
GBCM0 *(Control)*	2450.5	Moderate	Baseline
GBCM1	1820.4	Low	-25.7 %
GBCM2	1945.1	Low	-20.6 %
GBCM3	2110.8	Moderate	-13.9 %
GBCM4	2350.2	Moderate	- 4.1 %
GBCM5	2680.0	Moderate	+9.4 %
GBCM6	1650.3	Low	-32.7 %
GBCM7 *(Optimum)*	1493.1	Low	-39.1 %
GBCM8	2020.6	Low	-17.5 %

The maximum charge passed (2680 Coulombs) was achieved for GBCM5 (100 % fly ash). This indicates that GBCM5 has the lowest resistance to chloride ion penetration of all the mixes tested. The poor performance of GBCM5 was attributed to the relatively slow fly ash geopolymerization under ambient curing condition, resulting in a relatively porous matrix that allowed chloride ion transport. However, much lower values of charge passed of 1945.1 C and 1493.1 C were obtained for GBCM2 (75% GGBFS + 25% fly ash) and GBCM7 (50% GGBFS + 50% WGP) respectively indicating significant improvement in resistance to chloride ingress. The values indicate the low chloride ion penetrability as per ASTM C1202 and dense and less permeable geopolymer matrix formation [32,36]. The increased durability of GBCM2 and GBCM7 is attributed to the synergistic effect of precursor materials and bacterial biomineralization. The high calcium of GGBFS was

beneficial for the formation of C-(A)-S-H gel and the reactive silica from the fly ash and waste glass powder was beneficial for the formation of N-A-S-H gel, which led to a finer pore structure [27,35]. The CFU analysis also confirmed the viability of the Exiguobacterium aurantiacum that facilitated microbial induced calcium carbonate precipitation (MICP) to fill the microvoids and capillary pores, thus reducing the connectivity of the permeable pathways available for chloride ion migration. GBCM4 exhibited higher charge passed value of 2350.2 Coulombs indicating moderate chloride penetrability. The increase in fly ash content and decrease in GGBFS proportion could have hindered the formation of geopolymer gel which resulted in a comparatively less dense matrix than the optimized mixes. The other mixtures GBCM0, GBCM3, GBCM6 and GBCM8 presented moderate permeability to chlorides. This is because of the effect of different proportions of GGBFS, fly ash and WGP on the refinement of matrix and pore connectivity. Finally, the RCPT results show that the precursor formulation has a significant effect on the resistance to chloride penetration. The formation of denser geopolymer matrix resulted in a significant reduction of chloride permeability when using GGBFS and waste glass powder. In addition, the bacterial CaCO3 precipitation was used to fill the pores and micro-cracks to improve the durability. The lowest passing charge was observed for GBCM2 while the best overall mechanical and durability performance was observed for GBCM7 indicating that the binder composition of 50% GGBFS-50% WGP has an optimum balance between strength development and resistance to chloride ingress [36,37]. These findings are in line with previous studies in which significant improvement of the durability of alkali activated concretes was observed by increasing the gel formation and the matrix densification by using GGBFS-based geopolymer binder and reactive waste glass powder.

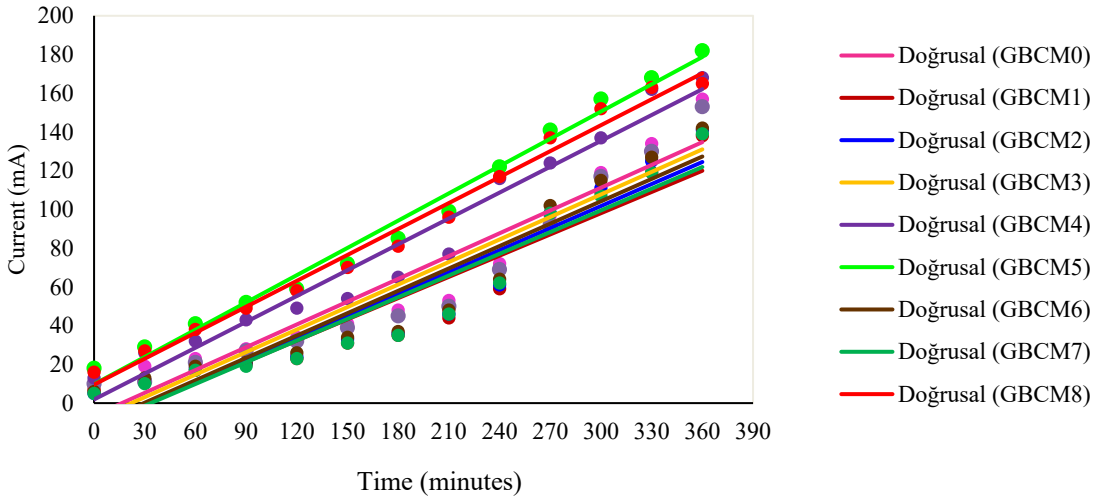


Fig. 10. Comparison of the RCPT values of bacterial geopolymer concrete

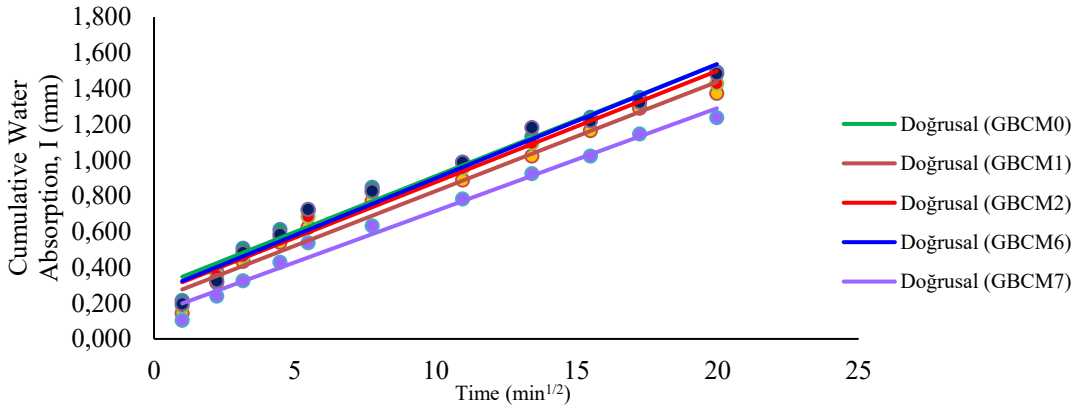
3.7 Sorptivity

The primary and secondary sorptivity results for bacteria-enhanced geopolymer concrete (BGPC) mixes at 28 days are shown in Fig. Fig. 11(a) and Fig. 11(b) respectively. The rate of water absorption in the first 6 h (primary sorptivity, Si) and between day 1 and day 7 (secondary sorptivity, Ss) was determined as the slope of the respective linear regressions and is summarized in Table 6, along with its correlation coefficients (Ri^2 and Rs^2). The sorptivity is an important durability parameter to assess the capillary water absorption through interconnected pores. Lower value of sorptivity means denser microstructure and better resistance against water intrusion. In all the mixtures, a linear relation between the cumulative water absorption and the square root of time was observed, which confirm that the water transport was essentially controlled by the capillary suction in the primary and secondary absorption phases. During the primary phase of sorptivity the maximum rate of water absorption was observed for control concrete (GBCM0) and minimum sorptivity was observed for GBCM7 (50% GGBFS + 50% WGP) during the test duration. The GBCM7 curve has a flatter slope, indicating a lower rate of capillary water absorption, which suggests a more refined pore structure and lower pore connectivity. The binary GGBFS mix

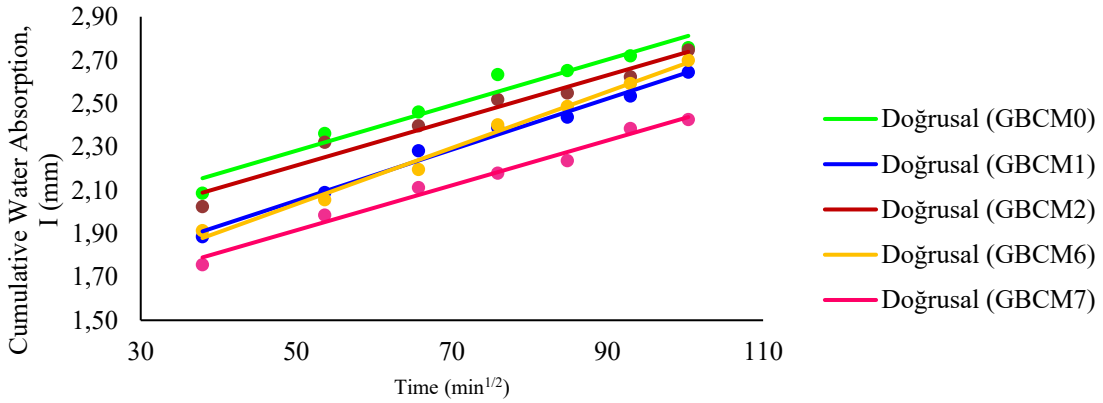
(GBCM1) and the ternary mixture with GGBFS, fly ash and WGP (GBCM6) showed lower sorptivity than the control mix and GBCM2 showed an intermediate behavior. The results showed that the addition of GGBFS and WGP can significantly reduce the permeability of the geopolymer matrix. GBCM7 had the lowest value of secondary sorptivity followed by GBCM6 and GBCM1. But the rate of water absorption was slower than that of the first stage. On the other hand, GBCM0 exhibited the highest sorptivity value in the test, which indicates higher interconnectivity of pores and increased susceptibility to moisture ingress.

Table 6. Primary (Si) and secondary (Ss) Sorptivity coefficients and correlation factors (R2) at 28 days

Mix ID	Primary Sorptivity S_i ($mm/min^{0.5}$)	R^2 (Primary)	Secondary Sorptivity S_s ($mm/min^{0.5}$)	R^2 (Secondary)	Reduction in S_i vs. Control (%)
GBCM0	0.0388	0.989	0.0165	0.982	-
GBCM1	0.0352	0.991	0.0148	0.985	9.3 %
GBCM2	0.0361	0.987	0.0151	0.981	7.0 %
GBCM3	0.0375	0.985	0.0158	0.979	3.4 %
GBCM4	0.0392	0.982	0.0169	0.976	-1.0 %
GBCM5	0.0421	0.978	0.0182	0.972	-8.5 %
GBCM6	0.0358	0.990	0.0150	0.984	7.7 %
GBCM7	0.0341	0.994	0.0141	0.988	12.1 %
GBCM8	0.0379	0.984	0.0161	0.978	2.3 %



(a) Primary Sorptivity @ 28 days



(b) Secondary Sorptivity @ 28 days

Fig. 11. Sorptivity vs square root of time at 28 days

The optimized geopolymer mixes exhibited lower sorptivity, implying that the pore structure was still capable of hindering water movement after the initial capillary pores were filled. The better sorptivity performance of GBCM7 is attributed to the synergy effect of GGBFS and waste glass

powder. The high calcium in GGBFS contributed to the formation of C-(A)-S-H gel, while the reactive amorphous silica in WGP promoted the formation of N-A-S-H gel, resulting in a dense and uniform geopolymer matrix. The CFU analysis also validated the viability of Exiguobacterium aurantiacum, which led to microbial-induced calcium carbonate precipitation (MICP) to fill the capillary pores and microcracks, and thereby diminished the continuity of water transport pathways. The formation of the geopolymer gel and the bacterial biomineralization gave rise to a significant reduction of the water absorption of the capillaries [38,39]. The sorptivity results are in agreement with the results of compressive strength, split tensile strength, flexural strength and rapid chloride penetration test which confirms that the mixtures with lower pore connectivity showed better mechanical properties and durability. Among all the mixes studied, the GBCM7 mix had lowest sorptivity and the best overall performance, which indicates the effectiveness of 50% GGBFS–50% WGP binder system in matrix densification and durability improvement. The results obtained are in agreement with previous studies reporting that the addition of GGBFS and waste glass powder improves the pore structure of alkali activated materials, while bacterial MICP further reduces the water absorption by pore filling and micro-structural densification.

3.8 Microstructure Analysis

The SEM micrographs of the control concrete (GBCM0) and optimum bacteria-enhanced geopolymer concrete (GBCM7) are shown in Figure 12, and the corresponding EDS spectrum is presented in Figure 13.

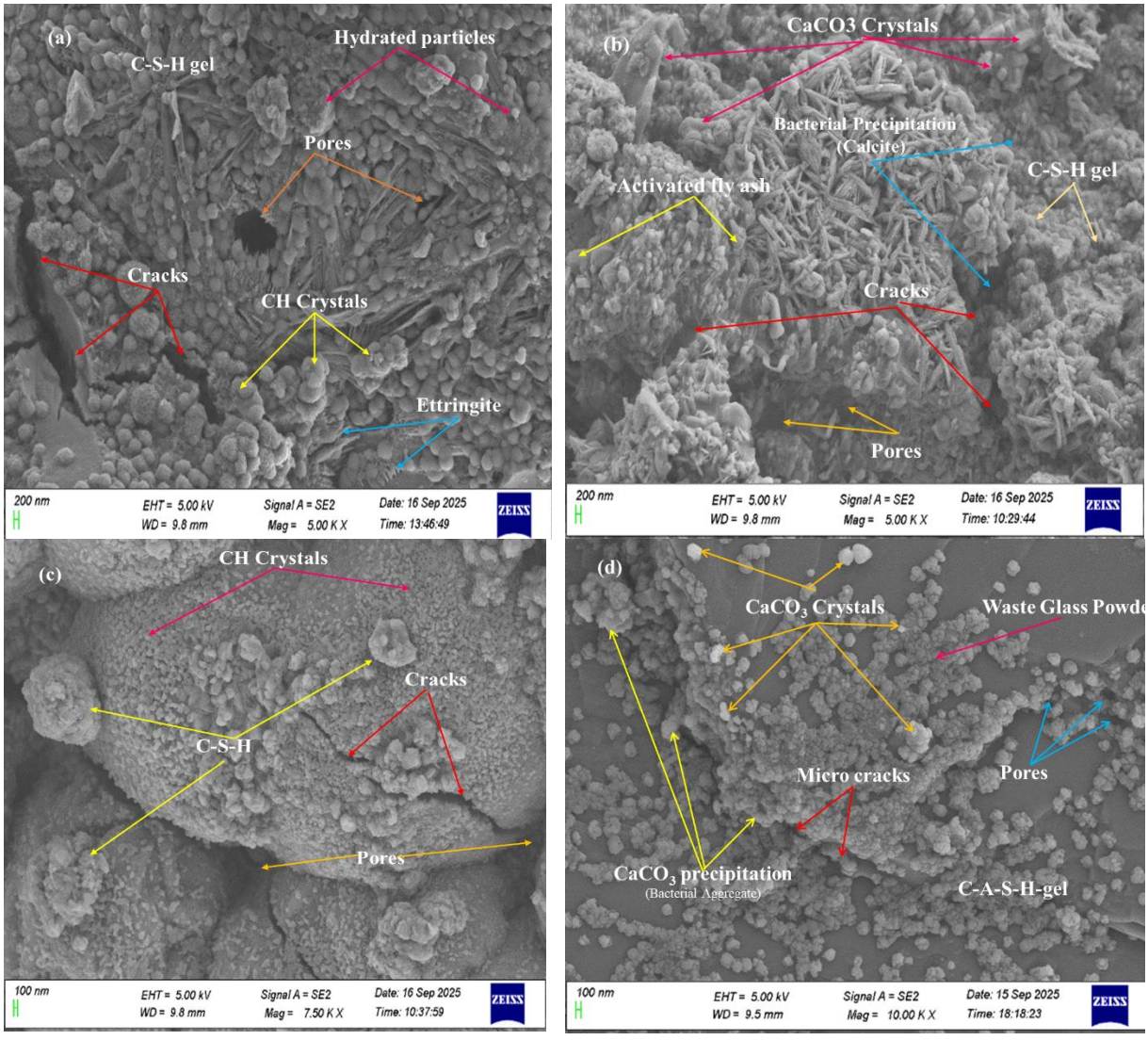


Fig. 12. SEM Images of the Fracture Surface; (a) & (c) shows reference concrete mix (GBCM0), and (b) & (d) shows GBCM7 mix

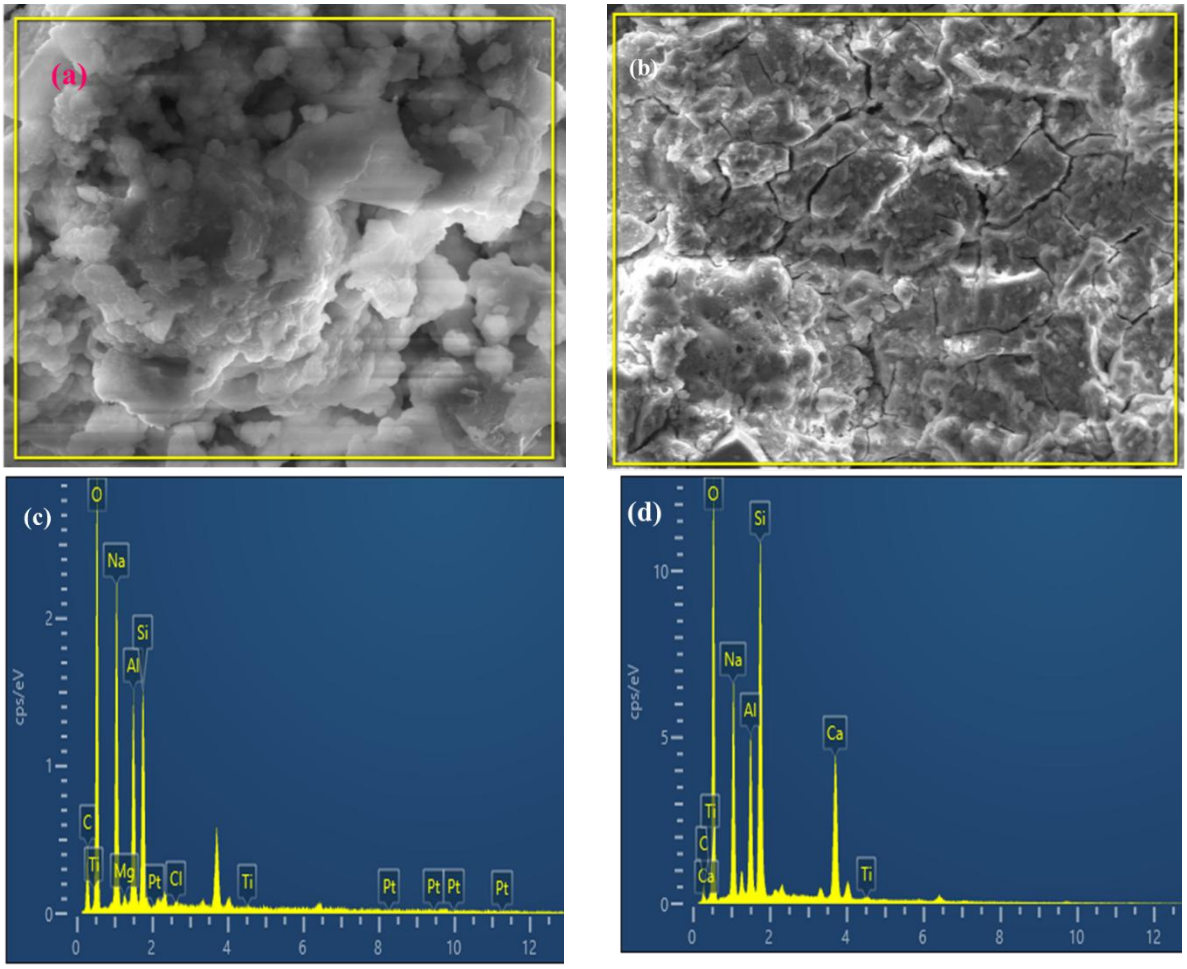


Fig. 13. SEM Images and EDS of the Fracture Surface; (a) & (c) Reference concrete mix (GBCM0), and (b) & (d) Optimum concrete mix (GBCM7)

The effect of precursor composition and bacterial activity on the morphology of geopolymer matrix was studied on fractured specimens which exhibited the highest compressive strength after mechanical testing. The SEM image of the control concrete (GBCM0) displays a relatively heterogeneous microstructure with visible pores, microcracks and partially hydrated cementitious products. The presence of these defects signifies that the matrix densification is incomplete, providing interconnected pathways for water and chloride ion transport. These results are consistent with the lower values of compressive, split tensile and flexural strengths and higher values of sorptivity and chloride permeability of control mixture [40]. However, SEM image of GBCM7 reveals a dense and compact microstructure with high formation of geopolymer gel and lesser number of pores and microcracks.Clearly visible in the matrix showing active microbial induced calcium carbonate precipitation (MICP) are needle-like and rhombohedral crystalline deposits identified as calcium carbonate [32,33]. The CFU analysis confirming the viability of Exiguobacterium aurantiacum corroborated the formation of these biominerals during curing. The precipitated calcite was successfully filling the internal voids and microcracks, making the matrix more homogeneous and improving the bond between the geopolymer paste and aggregates. Furthermore, a large amount of C-(A)-S-H gel coexisting with the bacterial calcite deposits is also observed, which is indicative of the synergistic interaction between the geopolymerization and biomineralization resulting in improved densification of the matrix. The improved microstructure of GBCM7 can also be attributed to the simultaneous addition of 50% GGBFS and 50% waste glass powder. The high content of calcium in GGBFS promoted the formation of the calcium-rich reaction products and the amorphous silica released from the waste glass powder promoted the formation of additional geopolymer gels. Therefore, the optimized binder composition offered a continuous and compact geopolymer network with reduced pore connectivity, which is responsible for the superior mechanical properties and durability of GBCM7. Moreover, the EDS spectrum of GBCM7

confirms the formation of the geopolymer reaction products. Strong peaks for oxygen (O), silicon (Si), aluminum (Al), calcium (Ca), sodium (Na) and carbon (C) were observed, indicating the presence of aluminosilicate gels and calcium rich binding phases. Strong peaks of calcium and carbon suggest the precipitation of calcium carbonate. Peaks of silicon and aluminum confirm the formation of the geopolymer aluminosilicate gels. The sodium is derived from the alkaline activator solution and the small titanium (Ti) peak is due to trace mineral constituents of the raw materials. These elements confirm the simultaneous formation of C-(A)-S-H/N-A-S-H gels and bacterial calcite within the geopolymer matrix. In summary, the results of the mechanical and durability tests are supported by SEM and EDS analyses. The higher compressive strength, split tensile strength, flexural strength, lower sorptivity and better resistance to chloride ion penetration of GBCM7 are due to the dense microstructure, less pore volume, high amount of geopolymer gel and bacterial calcium carbonate precipitation. It should be noted that some fine microcracks observed in the SEM images do not exclusively represent intrinsic matrix distress, but are partially attributed to localized desiccation shrinkage induced by the high vacuum condition and high energy electron beam exposure during SEM sample preparation and platinum sputter coating. The results indicate that the combined application of GGBFS, waste glass powder and viable Exiguobacterium aurantiacum significantly improves the microstructural integrity of the geopolymer concrete, resulting in enhanced long-term performance.

3.9 Fourier Transform Infrared Spectroscopy (FTIR)

The FTIR spectra of control concrete (GBCM0), bacteria-enhanced GGBFS geopolymer concrete (GBCM1) and optimum bacteria-enhanced geopolymer concrete containing 50% GGBFS and 50% waste glass powder (GBCM7) are shown in Fig. 14. The spectra were analyzed to identify the reaction products formed during geopolymerization and to evaluate the influence of bacterial incorporation and waste glass powder on the chemical structure of the geopolymer matrix. The broad absorption band found for all mixtures in the range of 3200–3600 cm−1 is due to the stretching vibration of O–H bonds related to the physically adsorbed water and hydroxyl groups. The band's existence points to the formation of hydrated reaction products in the geopolymer matrix. The weak band at 1600–1650 cm−1 is attributed to the bending vibration of H–O–H molecules, confirming the presence of bound water in the hydration products. All specimens exhibited a characteristic absorption band in the range of 900–1200 cm−1 corresponding to asymmetric stretching vibration of Si–O–T (T = Si or Al) bonds, which represents the formation of aluminosilicate geopolymer gels. In contrast, GBCM1 and GBCM7 showed a significantly higher intensity of this band compared to control concrete, showing improved geopolymerization due to incorporation of GGBFS and waste glass powder. The increase in intensity indicates that more C-(A)-S-H and N-A-S-H gels are formed, which are the main reason for the improved strength and matrix densification shown by these mixtures. The geopolymer mixtures treated with bacteria, especially GBCM7, showed a higher intensity of absorption bands at approximately 1400 cm^{-1} and 700 cm^{-1}. These bands are due to carbonate (CO3 2-) vibration of calcium carbonate (calcite) which confirms the occurrence of microbial induced calcium carbonate precipitation (MICP) [41]. The CFU analysis confirms the viability of the Exiguobacterium aurantiacum and supports the formation of these calcite deposits during curing. The precipitated CaCO3 occupied the pores and microcracks thus refining the pore structure and improving the mechanical strength and durability of the geopolymer concrete. The spectrum of GBCM7 showed stronger Si–O–T and carbonate absorption bands than GBCM1, indicating that the simultaneous incorporation of GGBFS and waste glass powder not only induced more geopolymer gel formation but also improved bacterial biomineralization. The reactive amorphous silica released from the waste glass powder was involved in secondary geopolymerization reactions that resulted in a denser aluminosilicate network. This is consistent with the SEM analysis in which a dense microstructure with high content of geopolymer gel and calcite crystals was observed in GBCM7. The increased chemical bonding observed from FTIR thus correlates with higher compressive, split tensile and flexural strengths, and lower sorptivity and chloride permeability of the optimized mix. Overall, FTIR analysis confirms that the incorporation of GGBFS, waste glass powder and viable Exiguobacterium aurantiacum changed significantly the chemical composition of the geopolymer matrix, promoting the formation of C-(A)-S-H/N-A-S-H gels and bacterial calcium carbonate. These reaction products

form a denser and chemically stable matrix, which explains the better mechanical performance and durability of GBCM7 compared to the control concrete. The results of FTIR are in good agreement with SEM, EDS, sorptivity and rapid chloride penetration results indicating the beneficial role of bacterial biomineralization and waste glass powder in improving the microstructure of geopolymer concrete.

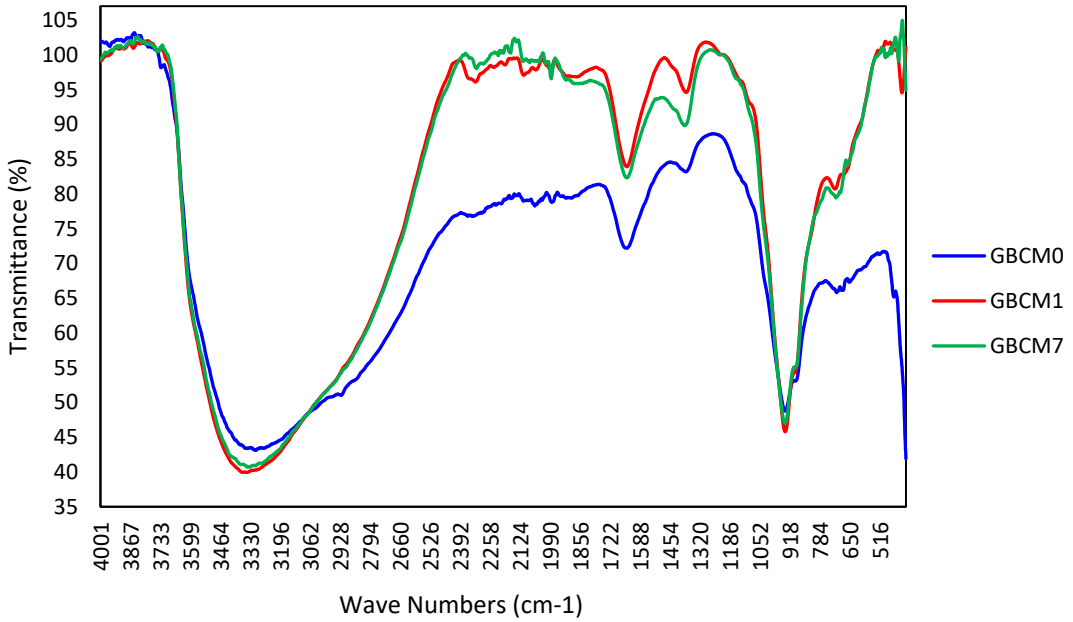


Fig. 14. FTIR spectrum of reference concrete and bacterial geopolymer concrete

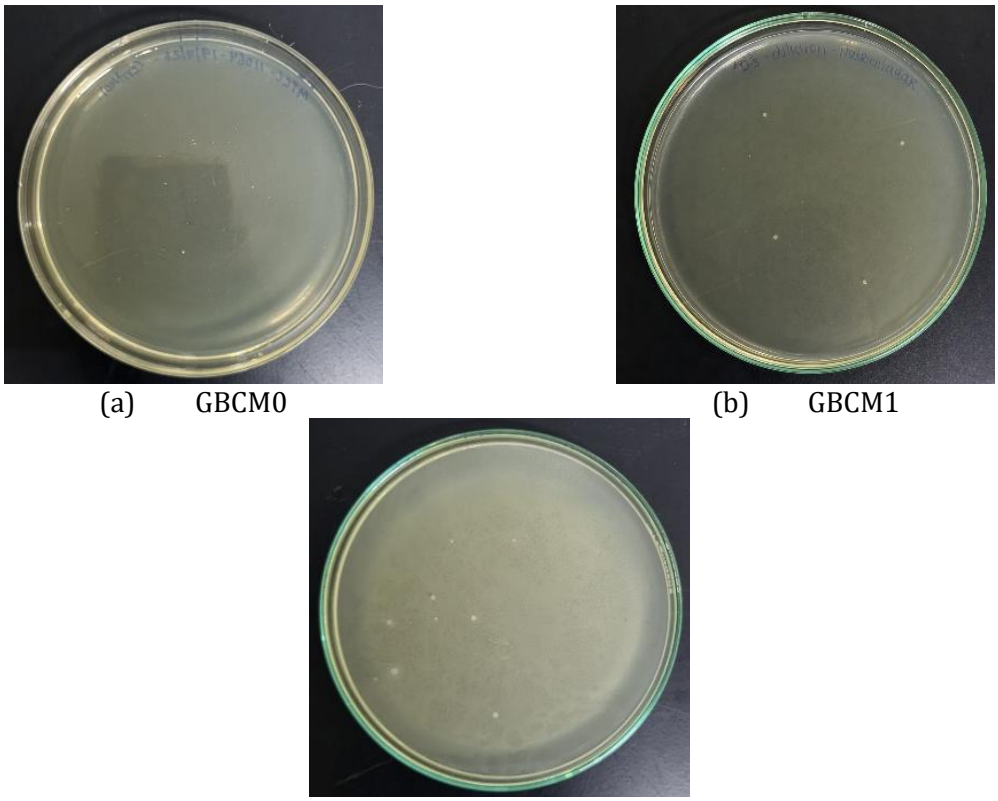
3.10 Colony Forming Units (CFU) Assay

Table 7. Colony forming units (CFU) test results

Mix ID	CFU (CFU/g)		
	Day 0	Day 28	Day 90
GBCM0	0	0	0
GBCM1	1.0×10^6	1.8×10^5	4.0×10^4
GBCM7	1.0×10^6	2.3×10^5	5.0×10^4

CFU quantification was performed on three representative mixtures GBCM0 (OPC Control), GBCM1 (100% GGBFS reference geopolymer), and GBCM7 (optimal 50% GGBFS + 50% WGP geopolymer) to evaluate survival across distinct matrix chemical environments without redundant analysis of intermediate ratios. The viability of Exiguobacterium aurantiacum in hardened geopolymer concrete ambient curing was assessed by the colony-forming unit (CFU) method, and the results are shown in Table 7. No bacterial colonies were observed in the control mixture (GBCM0), indicating that there was no bacterial contamination during the preparation and testing of the specimens. In contrast, viable bacterial colonies were recovered from the bacteria-incorporated hardened geopolymer concrete, indicating that E. aurantiacum survived within the highly alkaline geopolymer matrix even though it was directly incorporated into the concrete. The mixtures containing incorporated bacteria exhibited the viable cell populations of 4.0×10^4 CFU/g for GBCM1 and 5.0×10^4 CFU/g for GBCM7. Because colony counts on high-dilution plates were low (4–5 colonies/plate), random sampling variability is higher than standard counting ranges (30–300 CFU/plate). This is recognized as a statistical limitation of testing hardened, dense concrete matrices. Recovery of viable bacterial cells after 90 days indicates that a fraction of the bacterial population remained active within the hardened geopolymer matrix. The slight difference in CFU values between the mixtures might be attributed to the differences in the composition of the geopolymer matrix and the pore characteristics that determine the local environment for the bacteria to survive. As bacterial viability declined after prolonged exposure to the alkaline matrix, the remaining viable cells demonstrate E. aurantiacum's ability to tolerate the geopolymer

environment [42] the urease enzyme hydrolyzed urea and promoted carbonate generation. The presence of viable bacteria favors the occurrence of microbial-induced calcium carbonate precipitation (MICP), which can promote pore refinement and matrix densification. The calcium carbonate produced by the metabolic activity of bacteria can reduce the pore connectivity and microvoids of bacteria-enhanced geopolymer concrete, thus enhancing the mechanical strength and durability of bacteria-enhanced geopolymer concrete. Fig. 15. Shows the comparison of CFU plates of control and bacterial geopolymer concrete specimens.



(a) GBCM0 (b) GBCM1

(c) GBCM7

Fig. 15. Comparison of CFU plates of control and bacterial geopolymer concrete specimens

3.11 Urease Activity Assay

The urease activity of Exiguobacterium aurantiacum was measured to assess the metabolic activity of the bacterial culture into hardened geopolymer concrete. The results are shown in Fig. 16. Original in-house experimental characterization showed that Exiguobacterium aurantiacum exhibits a rapid exponential phase between 6 and 18 h at 37 °C, reaching stationary density (OD600 approx. 1.25) at 24 h. Urease activity assaying confirmed sustained activity of 0.85±0.04 U/mL across alkaline conditions (pH 10.0–11.5), verifying its suitability for geopolymer biomineralization. The control mixture (GBCM0) had a very low level of urease (0.3 mg/5 mL) and no enzymatic activity of bacteria. However, the mixtures incorporated with bacteria showed a significant increase in urease activity. The GBCM1 and GBCM7 were 20.3 mg/5 mL and 24.8 mg/5 mL, respectively. The higher urease activity in GBCM7 indicates an increased bacterial metabolism. In the highly alkaline geopolymer matrix, biomineralization does not rely on microbial pH elevation. Instead, Exiguobacterium aurantiacum produces extracellular urease enzymes that catalyze the enzymatic hydrolysis of urea into ammonium (NH4+) and carbonate (CO32-) ions via Eq. (3):

$$CO(NH2)2 + 2H2O \xrightarrow{Urease} 2NH4+ + CO32- \quad (3)$$

The generated carbonate ions react spontaneously with free Ca2+ ions provided by dissolved calcium lactate and GGBFS to precipitate micro-crystalline calcite (CaCO3) within matrix voids:

$$Ca2+ + CO32- \rightarrow CaCO3\downarrow \quad (4)$$

Consequently, the elevated urease activity observed in GBCM7 confirms robust bacterial metabolic efficiency, driving greater biomineralization potential directly within remnant gel micropores. The GBCM7 with higher urease activity had a higher mechanical strength and durability of the mix. The calcium carbonate deposition in the pores and microvoids improves the pore structure and the interfacial bonding in the geopolymer matrix. Thus, the increased enzymatic activity of E. aurantiacum results in matrix densification, reduction in permeability and overall improved performance of bacteria enhanced geopolymer concrete.

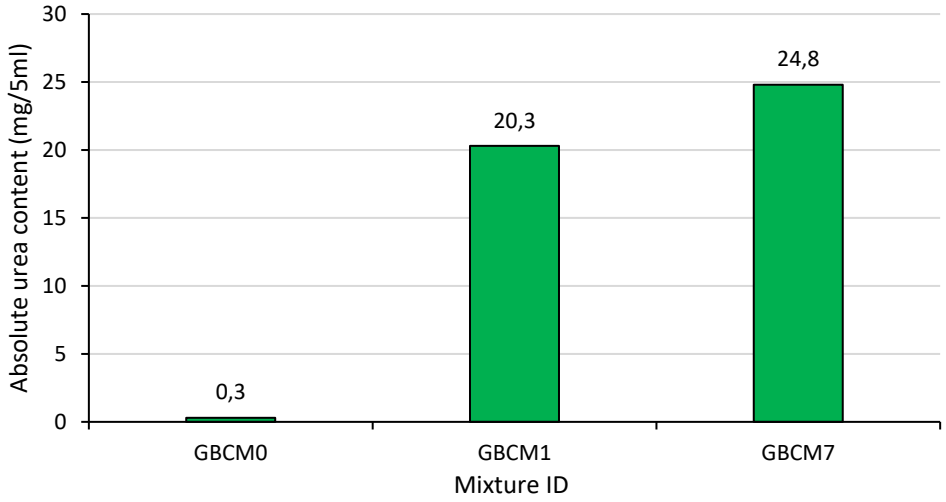


Fig. 16. Comparison of urease activity test values of bacterial geopolymer concrete

4. Conclusions

The effect of waste glass powder (WGP) as an auxiliary geopolymer precursor on mechanical, durability, bacterial and microstructural properties of bacteria-enhanced geopolymer concrete incorporating ground granulated blast furnace slag (GGBFS), fly ash and Exiguobacterium aurantiacum was studied in the present work. Based on the experimental results, we can conclude that:

- Bacteria-enhanced geopolymer concrete showed excellent performance when WGP was added under ambient curing conditions. The geopolymer concrete with 50% GGBFS and 50% WGP (GBCM7) was observed to exhibit the best overall performance among the mixtures investigated. This is due to the synergistic effect of calcium-rich GGBFS, silica-rich WGP and bacterial biomineralization.
- The optimum blend (GBCM7) was found to give the best mechanical performance with compressive strength of 59.00 MPa at 28 days and 73.75 MPa at 90 days, with corresponding improvements in split tensile strength of 5.66 MPa at 90 days and flexural strength of 6.01 MPa at 90 days than control blend. The enhancements are due to the formation of a thicker geopolymer matrix and the improvement of interfacial bonding by the synergistic effect of geopolymerization and microbial-induced calcium carbonate precipitation (MICP). In rapid chloride permeability testing (ASTM C1202), GBCM7 recorded a total charge passed of 1493.1 C (Low Permeability), demonstrating a 39.1% reduction in charge passed compared to the OPC control mix GBCM0 (2450.5 C).
- The bacterial viability analysis (CFU) showed that Exiguobacterium aurantiacum was able to survive and biomineralize in the geopolymer conditions as it survived during the curing period in the highly alkaline geopolymer matrix.
- The urease activity test indicated the metabolic activity of Exiguobacterium aurantiacum in the geopolymer system. Active urease enzyme catalyzed urea hydrolysis and microbiologically induced calcium carbonate precipitation resulted in pore refinement, crack filling and matrix densification by calcite formation.
- The durability performance of geopolymer concrete was greatly enhanced by the addition of WGP and bacterial biomineralization. The optimized mixture exhibited lower water

absorption and sorptivity and higher surface resistivity indicating lower connectivity of pores and better resistance to moisture and ionic ingress.

- Microstructural analysis was performed by SEM and FTIR, revealing the formation of a compact geopolymer matrix and formation of a large number of reaction products and biologically induced CaCO3 crystals. The co-existence of C-(A)-S-H and N-(C)-A-S-H gels with precipitation of calcite is effective to reduce the microcracks and the pore volume which results in the improvement of the mechanical strength and long-term durability.
- The increase in WGP content enhanced the availability of silica, but the availability of reactive calcium required for effective geopolymerization decreased with excessive replacement of GGBFS, which caused a slight decrease in the mechanical and durability performance beyond the optimum replacement level. Therefore, the optimum ratio of GGBFS and WGP is required for maximum performance of bacteria-enhanced geopolymer concrete.

The primary limitation of this study is the absence of a parallel bacteria-free geopolymer control series across all replacement levels, which precludes isolating the exact quantitative contribution of MICP relative to pure geopolymerization. Additionally, high-vacuum SEM imaging introduces localized microcracking, and low CFU plate counts from dense matrix extractions increase statistical variance. The combined use of GGBFS, fly ash, waste glass powder and Exiguobacterium aurantiacum is an eco-friendly and efficient way to develop high-performance geopolymer concrete with superior mechanical properties, improved durability and microstructure, and encouraging the beneficial application of industrial by-products. The potential of the proposed material for low-carbon and durable structural applications is discussed. Future works should be oriented to long-term field performance of bacteria-enhanced geopolymer concrete under aggressive environmental conditions, life cycle assessment and large-scale structural validation for practical application in sustainable infrastructure.

References

[1] Huntzinger DN, Eatmon TD. A life-cycle assessment of Portland cement manufacturing: Comparing the traditional process with alternative technologies. Journal of Cleaner Production. 2009;17:668-675. https://doi.org/10.1016/j.jclepro.2008.04.007

[2] Taha B, Nounu G. Properties of concrete contains mixed color waste recycled glass as sand and cement replacement. Construction and Building Materials. 2008;22:713-720. https://doi.org/10.1016/j.conbuildmat.2007.01.019

[3] Jonkers HM, Thijssen A, Muyzer G, Copuroglu O, Schlangen E. Application of bacteria as self-healing agent for the development of sustainable concrete. Ecological Engineering. 2010;36:230-235. https://doi.org/10.1016/j.ecoleng.2008.12.036

[4] Duan P, Yan C, Zhou W. Compressive strength and microstructure of fly ash based geopolymer blended with silica fume under thermal cycle. Cement and Concrete Composites. 2017;78:108-119. https://doi.org/10.1016/j.cemconcomp.2017.01.009

[5] Jindal BB, Patel PJ, Garg A. Effects of ultra-fine slag as mineral admixture on the compressive strength, water absorption and permeability of rice husk ash based geopolymer concrete. Materials Today: Proceedings. 2020;32:521-526. https://doi.org/10.1016/j.matpr.2020.04.219

[6] Bajpai R, Choudhary K, Srivastava A, Sangwan KS, Singh M. Environmental impact assessment of fly ash and silica fume based geopolymer concrete. Journal of Cleaner Production. 2020;254:120147. https://doi.org/10.1016/j.jclepro.2020.120147

[7] Rautray B, Rautray MSS. Performance of self-compacting geopolymer concrete using Bacillus licheniformis. Materials Today: Proceedings. 2020;33:5092-5098. https://doi.org/10.1016/j.matpr.2020.02.587

[8] Mahmood F, Ur Rehman SK, Jameel M, Khushnood RA, Rizwan SA. Self-healing bio-concrete using Bacillus subtilis encapsulated in iron oxide nanoparticles. Construction and Building Materials. 2022;323:126581. https://doi.org/10.3390/ma15217731

[9] Bayati M, Mohammad LAS. Efficiency of bacteria based self-healing method in alkali-activated slag (AAS) mortars. Journal of Building Engineering. 2021;43:103185. https://doi.org/10.1016/j.jobe.2021.102492

[10] Jaya Krishna GT, Niharika MNBLJ, Prasad PVSR. Experimental research of hybrid fibers based geo-polymer concrete. Materials Today: Proceedings. 2019;19:821-826.

[11] Turner LK, Collins FG. Carbon dioxide equivalent (CO2-e) emissions: A comparison between geopolymer and OPC cement concrete. Construction and Building Materials. 2013;43:125-130. https://doi.org/10.1016/j.conbuildmat.2013.01.023

[12] Yadav R, Saini PK, Chaudhari R. Enlargement of geo polymer compound material for the renovation of conventional concrete structures. Materials Today: Proceedings. 2021;45:3432-3438. https://doi.org/10.1016/j.matpr.2020.12.974
[13] Pasupathy K, Sanjayan J, Rajeev P, Law D, Kirubajiny L. The effect of chloride ingress in reinforced geopolymer concrete exposed in the marine environment. Journal of Building Engineering. 2021;44:102986. https://doi.org/10.1016/j.jobe.2021.102281
[14] Bureau of Indian Standards. IS 16714: Ground Granulated Blast Furnace Slag for Use in Cement, Mortar and Concrete - Specification. New Delhi, India: Bureau of Indian Standards; 2018.
[15] Bureau of Indian Standards. IS 3812 (Part 1): Pulverized Fuel Ash - Specification (Part 1: For Use as Pozzolana in Cement, Cement Mortar and Concrete). New Delhi, India: Bureau of Indian Standards; 2013.
[16] Bureau of Indian Standards. IS 383: Coarse and Fine Aggregate for Concrete - Specification. New Delhi, India: Bureau of Indian Standards; 2016.
[17] Bureau of Indian Standards. IS 252: Caustic Soda - Specification. New Delhi, India: Bureau of Indian Standards; 2013.
[18] Bureau of Indian Standards. IS 318: Sodium Silicate - Specification. New Delhi, India: Bureau of Indian Standards; 1995.
[19] Bureau of Indian Standards. IS 1070: Reagent Grade Water - Specification. New Delhi, India: Bureau of Indian Standards; 1992 (Reaffirmed 2003).
[20] Bureau of Indian Standards. IS 4031 (Part 4): Methods of Physical Tests for Hydraulic Cement (Determination of Consistency of Standard Cement Paste). New Delhi, India: Bureau of Indian Standards; 1988.
[21] Bureau of Indian Standards. IS 4031 (Part 5): Methods of Physical Tests for Hydraulic Cement (Determination of Initial and Final Setting Times). New Delhi, India: Bureau of Indian Standards; 1988.
[22] Bureau of Indian Standards. IS 516 (Part 1, Sec 1): Methods of Tests for Strength of Concrete (Determination of Compressive, Flexural, and Split Tensile Strength). New Delhi, India: Bureau of Indian Standards; 2021.
[23] Azhagarsamy S, Pannirselvam N, Premkumar R, Manivannan A, Sundararaman S, Kaliluthin AK. Mechanical and non-destructive evaluation of M30 grade concrete incorporating recycled ceramic waste as coarse aggregate: Experimental and statistical analysis. Research on Engineering Structures & Materials. 2025;11:1-17. https://doi.org/10.17515/resm2025-1079me0812rs
[24] ASTM International. ASTM C1202-12: Standard Test Method for Electrical Indication of Concrete's Ability to Resist Chloride Ion Penetration. West Conshohocken, PA: ASTM International; 2012.
[25] ASTM International. ASTM C1585-04: Standard Test Method for Measurement of Rate of Absorption of Water by Hydraulic-Cement Concretes. West Conshohocken, PA: ASTM International; 2004.
[26] Shi C, Wu Y, Riefler C, Wang H. Characteristics and pozzolanic reactivity of glass powders. Cement and Concrete Research. 2005;35:987-993. https://doi.org/10.1016/j.cemconres.2004.05.015
[27] Provis JL, van Deventer JSJ. Alkali Activated Materials: State-of-the-Art Report, RILEM TC 224-AAM. Dordrecht: Springer; 2014. https://doi.org/10.1007/978-94-007-7672-2
[28] Lu J, Poon C. Use of waste glass in alkali-activated and geopolymer materials: A review. Construction and Building Materials. 2018;160:399-415. https://doi.org/10.1016/j.conbuildmat.2017.11.080
[29] Le HT, Du K. Waste glass powder as cement replacement in concrete: A review. Cement and Concrete Composites. 2017;82:302-316.
[30] Le HT, Du K. Properties of high-volume glass powder concrete. Cement and Concrete Composites. 2017;75:22-29. https://doi.org/10.1016/j.cemconcomp.2016.10.010
[31] Rashad AM. A comprehensive overview about the influence of different additives on the properties of alkali-activated slag - A guide for civil engineering. Construction and Building Materials. 2013;47:29-55. https://doi.org/10.1016/j.conbuildmat.2013.04.011
[32] Bernal SA, Provis JL, Walkley B, San Nicolas R, Gehman JD, Brice DG, et al. Gel nanostructure in alkali-activated binders based on slag and fly ash, and effects of accelerated carbonation. Cement and Concrete Research. 2013;53:127-144. https://doi.org/10.1016/j.cemconres.2013.06.007
[33] De Muynck W, De Belie N, Verstraete W. Microbial carbonate precipitation in construction materials: A review. Ecological Engineering. 2010;36:118-136. https://doi.org/10.1016/j.ecoleng.2009.02.006
[34] Achal V, Mukherjee A, Reddy MS. Microbial concrete: Way to enhance the durability of building structures. Journal of Materials in Civil Engineering. 2011;23:730-734. https://doi.org/10.1061/(ASCE)MT.1943-5533.0000159
[35] Nath P, Sarker P. Effect of GGBFS on setting, workability and early strength properties of fly ash geopolymer concrete cured in ambient condition. Construction and Building Materials. 2014;66:163-171. https://doi.org/10.1016/j.conbuildmat.2014.05.080
[36] Albidah A, Al-Swaidani A, Al-Hadithi H. Durability performance of geopolymer concrete: A review. Polymers. 2022;14:868. https://doi.org/10.3390/polym14050868

[37] Singh B, Ishwarya G, Gupta M, Bhattacharyya SK. Geopolymer concrete: A review of some recent developments. Construction and Building Materials. 2015;85:78-90. https://doi.org/10.1016/j.conbuildmat.2015.03.036
[38] Hall C. Water sorptivity of mortars and concretes: A review. Magazine of Concrete Research. 1989;41:51-61. https://doi.org/10.1680/macr.1989.41.147.51
[39] Neville AM. Properties of Concrete. 5th ed. Harlow, UK: Pearson Education; 2011.
[40] Vishal M, Vishnupriyan M, Arumugam M, Nagarajan M. State-of-the-art review on the use of graphene oxide in enhancing mechanical properties and fire resistance of cementitious material. Journal of Structural Fire Engineering. 2026;17:62-83. https://doi.org/10.1108/JSFE-06-2025-0026
[41] Yao X, Zhang Z, Zhu H, Chen Y. Geopolymeric binder from fly ash and slag. Materials Letters. 2009;63:167-169.
[42] Vishnivetskaya TK, Kathariou S, Tiedje J. The genus Exiguobacterium: Global distribution, diversity, and biotechnological potential. Extremophiles. 2009;13:541-555. https://doi.org/10.1007/s00792-009-0243-5
[43] Dhami NK, Reddy MS, Mukherjee A. Biomineralization of calcium carbonates and their engineered applications: A review. Frontiers in Microbiology. 2013;4:314. https://doi.org/10.3389/fmicb.2013.00314
[44] Yang H, Liu L. A comprehensive overview of geopolymer composite: A bibliometric analysis and literature review. Case Studies in Construction Materials. 2022;16:e00830. https://doi.org/10.1016/j.cscm.2021.e00830
[45] Olivia M, Nikraz H. Properties of fly ash geopolymer concrete designed by Taguchi method. Materials & Design. 2012;36:191-198. https://doi.org/10.1016/j.matdes.2011.10.036
[46] Wang J, Van Tittelboom K, De Belie N, Verstraete W. Use of silica gel or polyurethane immobilized bacteria for self-healing concrete. Construction and Building Materials. 2012;26:532-540. https://doi.org/10.1016/j.conbuildmat.2011.06.054
[47] Wiktor V, Jonkers HM. Quantification of crack-healing in novel bacteria-based self-healing concrete. Cement and Concrete Composites. 2011;33:763-770. https://doi.org/10.1016/j.cemconcomp.2011.03.012
[48] Jonkers HM, Thijssen A, Muyzer G, Copuroglu O, Schlangen E. Application of bacteria as self-healing agent for development of sustainable concrete. Ecological Engineering. 2010;36:230-235. https://doi.org/10.1016/j.ecoleng.2008.12.036
[49] Reinhardt HW, Jooss M. Permeability and self-healing of cracked concrete as a function of temperature and crack width. Cement and Concrete Research. 2003;33:981-985. https://doi.org/10.1016/S0008-8846(02)01099-2
[50] Wang J, Soens H, Verstraete W, De Belie N. Self-healing concrete by use of microencapsulated bacterial spores. Cement and Concrete Research. 2014;56:139-152. https://doi.org/10.1016/j.cemconres.2013.11.009
[51] Wang J, Snoeck D, Van Vlierberghe S, Verstraete W, De Belie N. X-ray computed tomography proof of bacterial-based self-healing in concrete. Cement and Concrete Composites. 2014;53:289-304. https://doi.org/10.1016/j.cemconcomp.2014.07.014
[52] Bureau of Indian Standards. IS 7320: Specification for Concrete Slump Test Apparatus. New Delhi, India: Bureau of Indian Standards; 1974 (Reaffirmed 2018).
[53] Bureau of Indian Standards. IS 1199 (Part 2): Methods of Sampling and Analysis of Concrete (Determination of Consistency of Fresh Concrete). New Delhi, India: Bureau of Indian Standards; 1959.
[54] Bureau of Indian Standards. IS 516 (Part 1, Sec 1): Methods of Tests for Strength of Concrete (Determination of Compressive, Flexural, and Split Tensile Strength). New Delhi, India: Bureau of Indian Standards; 2021.
[55] Shetty MS. Concrete Technology: Theory and Practice. New Delhi, India: S. Chand & Company Ltd.; 2003.
[56] Neville AM. Properties of Concrete. 4th ed. New York, NY: John Wiley & Sons Inc.; 1997.
[57] Beglarigale A, Yildirim YSN, Yilmaz YD, Tanyildizi HT. Sodium silicate/polyurethane microcapsules used for self-healing in cementitious materials: Monomer optimization, characterization, and fracture behaviour. Construction and Building Materials. 2018;162:57-64. https://doi.org/10.1016/j.conbuildmat.2017.11.164
[58] Turner LK, Collins FG. Carbon dioxide equivalent (CO2-e) emissions: A comparison between geopolymer and OPC cement concrete. Construction and Building Materials. 2013;43:125-130. https://doi.org/10.1016/j.conbuildmat.2013.01.023
[59] Mors RMMHW, de Koster NHMJ, Mors GM, Jonkers HM, van Olst R, de Koster SAL. Geopolymer coating of bacteria-containing granules for use in self-healing concrete. Procedia Engineering. 2015;102:475-484. https://doi.org/10.1016/j.proeng.2015.01.193

[60] Jadhav UU, Zhang ML, Qian CJ, Eng BC, Yang EH. Viability of bacterial spores and crack healing in bacteria-containing geopolymer. Construction and Building Materials. 2018;169:716-723. https://doi.org/10.1016/j.conbuildmat.2018.03.039
[61] Schreiberova H, Bily P, Fladr J, Spacek K, Chylik R. Impact of the self-healing agent composition on material characteristics of bio-based self-healing concrete. Case Studies in Construction Materials. 2019;11:e00270. https://doi.org/10.1016/j.cscm.2019.e00250
[62] Kan L, Shi J, Dong B, Wu M. Self-healing of Engineered Geopolymer Composites prepared by fly ash and metakaolin. Cement and Concrete Research. 2019;125:105895. https://doi.org/10.1016/j.cemconres.2019.105895
[63] Garces JIT, Garces IJD, Beltran AB, Tan RR, Promentilla MAB. Life cycle assessment of self-healing geopolymer concrete. Cleaner Engineering and Technology. 2021;4:100147. https://doi.org/10.1016/j.clet.2021.100147
[64] Hareru WK, Harikrishnan S. Experimental study of the microstructural characterization of Microbial Induced Calcite Precipitation (MICP) bio-cement concrete. Iranian Journal of Science and Technology, Transactions of Civil Engineering. 2025;49:1193-1209. https://doi.org/10.1007/s40996-024-01652-x
[65] Alshalif AF, Nordin MIJ, Al-Gheethi OA, Khalid FS. Improvement of mechanical properties of bio-concrete using Enterococcus faecalis and Bacillus cereus. Environmental Engineering Research. 2019;24:630-637. https://doi.org/10.4491/eer.2018.306
[66] Mutitu DK, Wachira JM, Munji RM, Thiong'o JK, Munyao OM, Mwirichia MA, et al. Influence of Lysinibacillus sphaericus on compressive strength and water sorptivity in microbial cement mortar. Heliyon. 2019;5:e02881. https://doi.org/10.1016/j.heliyon.2019.e02881
[67] Ujwal SM, Sangwan KS, Goyal P, Sharma H, Nagabhushana SH, Parthasarathy P. Toward sustainable self-compacting concrete: Rheological, mechanical, durability, and microstructural evaluation of biomaterial-based cement substituents. Results in Engineering. 2025;27:103112. https://doi.org/10.1016/j.rineng.2025.106504
[68] Zamba DD, Duresa AM, Dubale YM, Mamo G, Tadesse HD. Strength and durability evaluation of bacteria-based self-healing concrete. Iranian Journal of Science and Technology, Transactions of Civil Engineering. 2025;49:1-13. https://doi.org/10.1007/s40996-025-01821-6
[69] Raichand R, Prakash S, Korpole N, Mayilraj SS. Exiguobacterium aquaticum sp. nov., a member of the genus Exiguobacterium. International Journal of Systematic and Evolutionary Microbiology. 2012;62:2150-2155. https://doi.org/10.1099/ijs.0.035790-0